Eur. Phys. J. C 25, 77–101 (2002)
Digital Object Identifier (DOI) 10.1007/s10052-002-0998-7

THE EUROPEAN PHYSICAL JOURNAL C

Small x phenomenology: summary and status

The Small x Collaboration

B. Andersson[1], S. Baranov[2], J. Bartels[3], M. Ciafaloni[4], J. Collins[5], M. Davidsson[6], G. Gustafson[1], H. Jung[6], L. Jönsson[6], M. Karlsson[6], M. Kimber[7], A. Kotikov[8], J. Kwiecinski[9], L. Lönnblad[1], G. Miu[1], G. Salam[10], M.H. Seymour[11], T. Sjöstrand[1], N. Zotov[12]

[1] Department of Theoretical Physics, Lund University, 223 52 Lund, Sweden
[2] Lebedev Institute of Physics, 117810 Moscow, Russia
[3] II. Institut für Theoretische Physik, Universität Hamburg, 22761 Hamburg, Germany
[4] Dipartimento di Fisica, Università di Firenze and INFN - Sezione di Firenze, 50125 Firenze, Italy
[5] Penn State University, 104 Davey Laboratory, University Park, PA 16802, USA
[6] Department of Physics, Lund University, 22 100 Lund, Sweden
[7] Department of Physics, University of Durham, Durham DH1 3LE, UK
[8] Bogoliubov Theoretical Physics Laboratory, Joint Institute for Nuclear Research, 141980 Dubna, Russia
[9] H. Niewodniczanski Institute of Nuclear Physics, 31-342 Krakow, Poland
[10] LPTHE, Universités P. & M. Curie (Paris VI) et Denis Diderot (Paris VII), Paris, France
[11] Theoretical Physics, Department of Physics and Astronomy, University of Manchester, M13 9PL Manchester, UK
[12] Skobeltsyn Institute of Nuclear Physics, Moscow State University, Moscow 119992, Russia

Received: 10 April 2002 /
Published online: 26 July 2002 –

Abstract. The aim of this paper is to summarize the general status of our understanding of small-x physics. It is based on presentations and discussions at an informal meeting on this topic held in Lund, Sweden, in March 2001.
This document also marks the founding of an informal collaboration between experimentalists and theoreticians with a special interest in small-x physics.
This paper is dedicated to the memory of Bo Andersson, who died unexpectedly from a heart attack on March 4th, 2002.

1 Introduction

In this paper we present a summary of the workshop on small-x parton dynamics held in Lund in the beginning of March 2001. During two days we went through a number of theoretical and phenomenological aspects of small-x physics in short talks and long discussions. Here we will present the main points of these discussions and try to summarize the general status of the work in this field.

For almost thirty years, QCD has been the theory of strong interactions. Although it has been very successful, there are still a number of problems which have not been solved. Most of these have to do with the transition between the perturbative and non-perturbative description of the theory. Although perturbative techniques work surprisingly well down to very small scales where the running coupling starts to become large, in the end what is observed are hadrons, the transition to which is still not on firm theoretical grounds. At very high energies another problem arises. Even at high scales where the running coupling is small the phase space for additional emissions increases rapidly and makes the perturbative expansion ill-behaved. The solution to this problem is to resum the leading logarithmic behavior of the cross section to all orders, thus rearranging the perturbative expansion into a more rapidly converging series.

The DGLAP [1–4] evolution is the most familiar resummation strategy. Given that a cross section involving incoming hadrons is dominated by diagrams where successive emissions are strongly ordered in virtuality, the resulting large logarithms of ratios of subsequent virtualities can be resummed. The cross section can then be rewritten in terms of a process-dependent hard matrix element convoluted with universal parton density functions, the scaling violations of which are described by the DGLAP evolution. This is called collinear factorization. Because of the strong ordering of virtualities, the virtuality of the parton entering the hard scattering matrix element can be neglected (treated collinear with the incoming hadron) compared to the large scale Q^2. This approach has been very successful in describing the bulk of experimental measurements at lepton–hadron and hadron–hadron colliders.

With HERA, a new kinematic regime has opened up where the very small x parts of the proton parton dis-

Table 1. Summary of the ability of the collinear and $k_\perp$-factorization approaches to reproduce the current measurements of some observables: OK means a satisfactory description; 1/2 means a not perfect but also a not too bad description, or in part of the phase space an acceptable description; OK? means satisfactory description if a heavy quark excitation component is added in leading order; NO means that the description is bad; and? means that no thorough comparison has been made

	collinear factorization	$k_\perp$-factorization
HERA observables		
high Q^2 D^* production	OK [8, 9]	OK [9, 10]
low Q^2 D^* production	OK [8, 9]	OK [9, 10]
direct photoproduction of D^*	1/2 [11]	OK [10, 12–15]
resolved photoproduction of D^*	NO [11]	1/2 [12–15]
high Q^2 B production	NO [16]	?
low Q^2 B production	NO [16]	?
direct photoproduction of B	OK? [17], NO [18]	OK [19–21]
resolved photoproduction of B	OK? [17]	OK [19–21]
high Q^2 di-jets	OK [22, 23]	?
low Q^2 di-jets	NO [22–25]	?
direct photoproduction of di-jets	1/2 [22, 24, 25]	?
resolved photoproduction of di-jets	NO [22, 24, 25]	?
HERA small-x observables		
forward jet production	NO [26]	OK [14]
forward π production	NO [26]	1/2 [27]
particle spectra	NO [28]	OK [14]
energy flow	NO [28]	?
photoproduction of J/Ψ	NO [29]	1/2 [30, 31]
J/Ψ production in DIS	NO	?
TEVATRON observables		
high-$p_\perp$ D^* production	?	?
low-$p_\perp$ D^* production	?	?
high-$p_\perp$ B production	OK? [32]	OK [20, 21, 33, 34]
low-$p_\perp$ B production	OK? [32]	OK [20, 21, 33, 34]
J/Ψ production	NO	?
high-$p_\perp$ jets at large rapidity differences	NO	?

tributions are being probed. The hard scale, Q^2, is not very high in such events and it was expected that the DGLAP evolution should break down. To some surprise, the DGLAP evolution has been quite successful in describing the strong rise of the cross section with decreasing x. For some non-inclusive observables there are, however, clear discrepancies as summarized in Table 1.

At asymptotically large energies, it is believed that the theoretically correct description is given by the BFKL [5–7] evolution. Here, each emitted gluon is assumed to take a large fraction of the energy of the propagating gluon, $(1-z)$ for $z \to 0$, and large logarithms of $1/z$ are summed up to all orders. Although the rise of F_2 with decreasing x as measured at HERA can be described with the DGLAP evolution, a strong power-like rise was predicted by BFKL. Just as for DGLAP, it is possible to factorize an observable into a convolution of process-dependent hard matrix elements with universal parton distributions. But as the virtuality and transverse momentum of the propagating gluon are no longer ordered, the matrix elements have to be taken off-shell and the convolution is also over transverse momentum with *unintegrated* parton distributions. We therefore talk about $k_\perp$-factorization [35, 36] or the semihard approach [37, 38].

Recently, the next-to-leading logarithmic (NLL) corrections to the BFKL equation were calculated and found

to be huge [39, 40]. This is related to the fact that at any finite energy, the cross section will also get contributions from emissions of gluons which take only a small fraction of the energy of the propagating gluon.

The CCFM [41–44] evolution equation resums also large logarithms of $1/(1-z)$ in addition to the $1/z$ ones. Furthermore it introduces angular ordering of emissions to correctly treat gluon coherence effects. In the limit of asymptotic energies, it is almost equivalent to BFKL [45–47], but also similar to the DGLAP evolution for large x and high Q^2. The cross section is still $k_\perp$-factorized into an off-shell matrix element convoluted with an unintegrated parton density, which now also contains a dependence on the maximum angle allowed in emissions.

An advantage of the CCFM evolution, compared to the BFKL evolution, is that it is fairly well suited for implementation into an event generator program, which makes quantitative comparison with data feasible also for non-inclusive observables. There exist today three such generators [14, 48–55] and they are all being maintained or/and developed by people from the departments of physics and of theoretical physics at Lund University.

Since 1998 there has been an on-going project in Lund, supported by the Swedish Royal Academy of Science, trying to get a better understanding of the differences between the different generators and to compare them to measured data. This project is what led up to the meeting in Lund in early March 2001, where a number of experts in the field were invited to give short presentations and to discuss the current issues in small-x physics in general and $k_\perp$-factorization in particular.

In this article we will try to summarize these discussions and give a general status report of this field of research. We also suggest the formation of an informal collaboration of researchers in the field, to facilitate a coherent effort to solve some of the current problems in small-x parton dynamics.

The outline of this article is as follows. First we give a general introduction to $k_\perp$-factorization in Sect. 2. Then, in Sect. 3, we discuss the off-shell matrix elements, both at leading order and the prospects of going to next-to-leading order. In Sect. 4, we discuss the unintegrated parton distributions and how they are evolved. Here we also try to quantify the transition between DGLAP and BFKL. We present a number of parameterizations of unintegrated parton distributions and make a few comparisons. Then we describe the next-to-leading logarithmic correction to the evolution. In Sect. 5 we describe the available event generators for small-x evolution. Finally in Sect. 6 we present our conclusions and discuss the forming of an informal collaboration to better organize the future investigations of small-x phenomenology.

2 The $k_\perp$-factorization approach

The calculation of inclusive quantities, like the structure function $F_2(x, Q^2)$ at HERA, performed in NLO QCD is in perfect agreement with the measurements. The NLO approach, although phenomenologically successful for $F_2(x, Q^2)$, is not fully satisfactory from a theoretical viewpoint because, in the words of Catani, *"the truncation of the splitting functions at a fixed perturbative order is equivalent to assuming that the dominant dynamical mechanism leading to scaling violations is the evolution of parton cascades with strongly ordered transverse momenta"* [56].

As soon as exclusive quantities like jet or heavy quark production are investigated, the agreement between NLO coefficient functions convoluted with NLO DGLAP parton distributions and the data is not at all satisfactory. Large so-called K-factors (normalization factors, for example $K = \frac{\sigma_{tot}}{\sigma_{NLO}}$) are needed to bring the NLO calculations close to the data [17, 18, 57, 58] ($K \sim 50$ for J/ψ production and $K \sim 2-4$ for bottom production at the

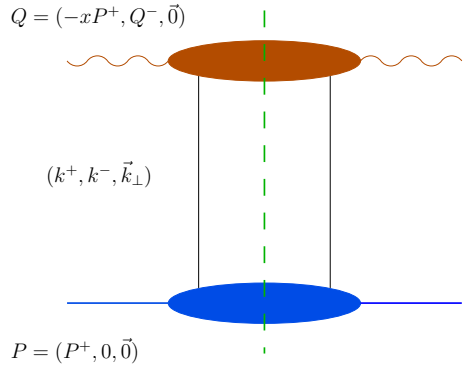

Fig. 1. Schematic picture of a typical unitarity diagram for deep inelastic scattering. An incoming proton with a large positive light-cone momentum, P^+, is being probed by a photon with a large virtuality and a large negative light-cone momentum. The photon scatters on a parton from the proton with space-like momentum k

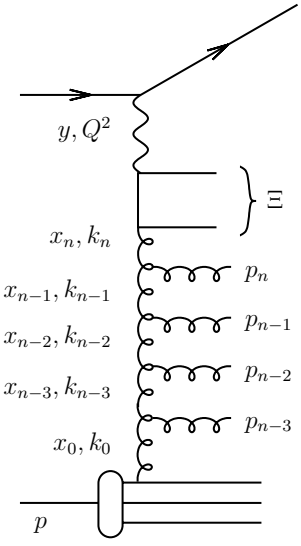

Fig. 2. Kinematic variables for multi-gluon emission. The t-channel gluon momenta are given by k_i and the gluons emitted in the initial state cascade have momenta p_i. The upper angle for any emission is obtained from the quark box, as indicated with Ξ. We define $z_{\pm i} = k_{\pm i}/k_{\pm(i\mp1)}$ and $q_i = p_{\perp i}/(1-z_{+i})$

TEVATRON), indicating that a significant part of the cross section is still missing in the calculations.

At small x the structure function $F_2(x, Q^2)$ is proportional to the sea quark density, which is driven by the gluon density. The standard QCD fits determine the parameters of the initial parton distributions at a starting scale Q_0. With the help of the DGLAP evolution equations these parton distributions are then evolved to any other scale Q^2, with the splitting functions still truncated at fixed $\mathcal{O}(\alpha_s)$ (LO) or $\mathcal{O}(\alpha_s^2)$ (NLO). Any physics process in the fixed order scheme is then calculated via collinear factorization into the coefficient functions $C^a(\frac{x}{z})$ and collinear (independent of $k_\perp$) parton density functions: $f_a(z, Q^2)$:

$$\sigma = \sigma_0 \int \frac{dz}{z} C^a(\frac{x}{z}) f_a(z, Q^2) \; . \tag{1}$$

At large energies (small x) the evolution of parton distributions proceeds over a large region in rapidity $\Delta y \sim \log(1/x)$ and effects of finite transverse momenta of the partons may become increasingly important. Cross sections can then be $k_\perp$ - factorized [35–38] into an off-shell ($k_\perp$ dependent) partonic cross section $\hat{\sigma}(\frac{x}{z}, k_\perp^2)$ and a $k_\perp$ - unintegrated parton density function $\mathcal{F}(z, k_\perp^2)$:

$$\sigma = \int \frac{dz}{z} d^2k_\perp \hat{\sigma}(\frac{x}{z}, k_\perp^2) \mathcal{F}(z, k_\perp^2) \; . \tag{2}$$

The unintegrated gluon density $\mathcal{F}(z, k_\perp^2)$ is described by the BFKL [5–7] evolution equation in the region of asymptotically large energies (small x). An appropriate description valid for both small and large x is given by the CCFM evolution equation [41–44], resulting in an unintegrated gluon density $\mathcal{A}(x, k_\perp^2, \bar{q}^2)$, which is a function also of the additional scale $\bar{q}$ described below. Here and in the following we use the following classification scheme: $x\mathcal{G}(x, k_\perp^2)$ describes DGLAP type unintegrated gluon distributions, $x\mathcal{F}(x, k_\perp^2)$ is used for pure BFKL and $x\mathcal{A}(x, k_\perp^2, \bar{q}^2)$ stands for a CCFM type or any other type having two scales involved.

By explicitly carrying out the $k_\perp$ integration in (2) one can obtain a form fully consistent with collinear factorization [56, 59]: the coefficient functions and also the DGLAP splitting functions leading to $f_a(z, Q^2)$ are no longer evaluated in fixed order perturbation theory but supplemented with the all-loop resummation of the $\alpha_s \log 1/x$ contribution at small x. This all-loop resummation shows up in the *Regge* form factor Δ_{Regge} for BFKL or in the *non-Sudakov* form factor Δ_{ns} for CCFM, which will be discussed in more detail in Sect. 4.

3 Off-shell matrix elements

It is interesting to compare the basic features of the $k_\perp$-factorization approach to the conventional collinear approach. In $k_\perp$-factorization the partons entering the hard scattering matrix element are free to be off-mass shell,

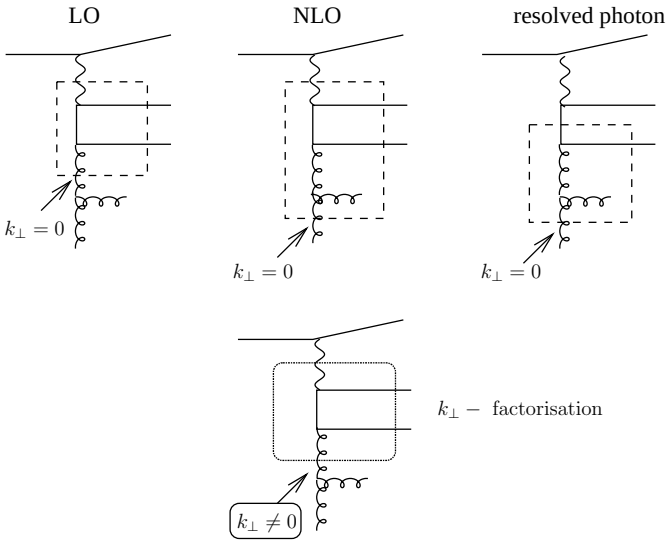

Fig. 3. Diagrammatic representation of LO, NLO and resolved photon processes in the collinear approach (top row) and compared to the $k_\perp$-factorization approach

in contrast to the collinear approach which treats all incoming partons massless. The full advantage of the $k_\perp$-factorization approach becomes visible, when additional hard gluon radiation to a $2 \to 2$ process like $\gamma g \to Q\bar{Q}$ is considered. If the transverse momentum $p_{\perp g}$ of the additional gluon is of the order of that of the quarks, then in a conventional collinear approach the full $\mathcal{O}(\alpha_s^2)$ matrix element for $2 \to 3$ has to be calculated. In $k_\perp$-factorization such processes are naturally included to leading logarithmic accuracy, even if only the LO α_s off-shell matrix element is used, since the $k_\perp$ of the incoming gluon is only restricted by kinematics, and therefore can aquire a virtuality similar to the ones in a complete fixed order calculation. In Fig. 3 we show schematically the basic ideas comparing the diagrammatic structure of the different factorization approaches. Not only does $k_\perp$-factorization include (at least some of the) NLO diagrams [60] it also includes diagrams of the resolved photon type, with the natural transition from real to virtual photons.

However, it has to be carefully investigated, which parts of a full fixed NLO calculation are already included in the $k_\perp$-factorization approach for a given off-shell matrix element and which are still missing or only approximatively included. It should be clear from the above, that the $\mathcal{O}(\alpha_s)$ matrix element in $k_\perp$-factorization includes fully the order $\mathcal{O}(\alpha_s)$ matrix element of the collinear factorization approach, but includes also higher order contributions. In addition, due to the unintegrated gluon density, also parts of the virtual corrections are properly resummed (Fig. 4b,c).

3.1 Order α_s off-shell matrix elements

Several calculations exist for the process $\gamma g \to Q\bar{Q}$ and $gg \to Q\bar{Q}$, where the gluon and the photon are both allowed to be off-shell [35, 36] and $Q(\bar{Q})$ can be a heavy or light quark (anti quark).

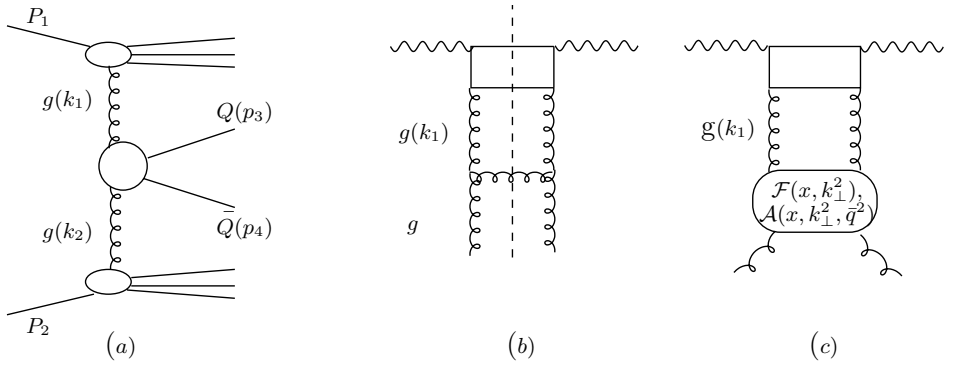

Fig. 4a–c. Schematic diagrams for $k_\perp$-factorization: **a** shows the general case for hadroproduction of (heavy) quarks. **b** shows the one-loop correction to the Born diagram for photoproduction **c** shows the all-loop improved correction with the factorized structure function $\mathcal{F}(x,k_\perp^2)$ or $\mathcal{A}(x,k_\perp^2,\bar{q}^2)$

The four-vectors of the exchanged partons k_1, k_2 (in Sudakov representation) are (Fig.4a):

$$k_1^\mu = z_1 P_1^\mu + \bar{z}_1 P_2^\mu + k_{\perp 1}^\mu \tag{3}$$
$$k_2^\mu = \bar{z}_2 P_1^\mu + z_2 P_2^\mu + k_{\perp 2}^\mu \tag{4}$$

with $z_i, \bar{z}_i$ being the two components $(+,-)$ of the light-cone energy fraction. The (heavy) quark momenta are denoted by p_3, p_4 and the incoming particles (partons) by P_1, P_2 with

$$P_{1,2} = \frac{1}{2}\sqrt{s}(\vec{0}, \pm 1, 1), \qquad 2P_1P_2 = s \tag{5}$$

where $\vec{0}$ indicates the vanishing two-dimensional transverse momentum vector. In the case of photoproduction or leptoproduction this reduces to:

$$k_1^\mu = P_1^\mu, \qquad k_2^\mu = k^\mu$$
photo-production (6)

$$k_1^\mu = q^\mu = yP_1^\mu + \bar{y}P_2^\mu + q_{\perp 2}^\mu, \qquad q^2 = -Q^2\ .$$
leptoproduction (7)

In all cases the off-shell matrix elements are calculated in the high energy approximation, with $\bar{z}_1 = \bar{z}_2 = 0$:

$$k_1^\mu = z_1 P_1^\mu + k_{\perp 1}^\mu \tag{8}$$
$$k_2^\mu = z_2 P_2^\mu + k_{\perp 2}^\mu, \tag{9}$$

which ensures that the virtualities are given by the transverse momenta, $k_1^2 = -k_{\perp 1}^2$ and $k_2^2 = -k_{\perp 2}^2$. The off-shell matrix elements involve 4-vector products not only with k_1, k_2 and the outgoing (heavy) quark momenta p_3, p_4, but also with the momenta of the incoming particles (partons) P_1, P_2. This is a result of defining the (off-shell) gluon polarization tensors in terms of the gluon (k_i) and the incoming particle vectors ($P_{1,2}$), which is necessary due to the off-shellness. In the collinear limit, this reduces to the standard polarization tensors. In [35, 36] it has been shown analytically, that the off-shell matrix elements reduce to the standard ones in case of vanishing transverse momenta of the incoming (exchanged) partons k_1, k_2.

Due to the complicated structure of the off-shell matrix elements, it is also necessary to check the positivity of the squared matrix elements in case of incoming partons which are highly off shell ($k_1^2, k_2^2 \ll 0$). It has been proven analytically in [61] for the case of heavy quarks with both incoming partons being off mass shell. We have also checked numerically, that the squared matrix elements are positive everywhere in the phase space, if the incoming particles (electron or proton) are exactly massless ($P_1^2 = P_2^2 = 0$). As soon as finite masses (of the electron or proton) are included, the exact cancellation of different terms in the matrix elements is destroyed, and unphysical (negative) results could appear.

From the off-shell matrix elements for a $2 \to 2$ process, it is easy to obtain the high energy limit of any on-shell 2(massless partons) $\to$ $2 + n$(massless partons) process, with $n = 1, 2$ (see Fig. 4b for the case of photoproduction), by applying a correction as given in [35, page 180]. By doing so, the corrections coming from additional real gluon emission are estimated (i.e. $\gamma g \to Q\bar{Q}g$ corrections to $\gamma g \to Q\bar{Q}$) with the incoming gluons now treated on-shell. In the case of hadroproduction one obtains the NNLO corrections $gg \to Q\bar{Q}gg$. In this sense $k_\perp$-factorization provides an easy tool for estimating K-factors in the high energy limit:

$$K = \frac{\sigma_{tot}}{\sigma(\text{LO or NLO})} \simeq \frac{\sigma(2 \to 2) + \sigma(2 \to 2 + n)}{\sigma(2 \to 2)} \tag{10}$$

In Table 2 we give an overview over the different off-shell matrix elements available. It has been checked, that the different calculations [35, 62] of the process $\gamma^{(*)}g^* \to Q\bar{Q}$ give numerically the same result. Also the matrix elements of [34–36] are identical.

3.2 Next-to-Leading corrections to α_s off-shell matrix elements

So far we have been dealing with matrix elements only in $\mathcal{O}(\alpha_s)$, but even here $k_\perp$-factorization has proven to be a powerful tool in the sense that it includes already in lowest order a large part of the NLO corrections [60] of the collinear approach. However, LO calculations are still subject to uncertainties in the scale of the coupling and in the normalization. As the next-to-leading corrections (including energy-momentum conservation) to the BFKL equation are now available also the matrix elements need to be calculated in the next-to-leading order.

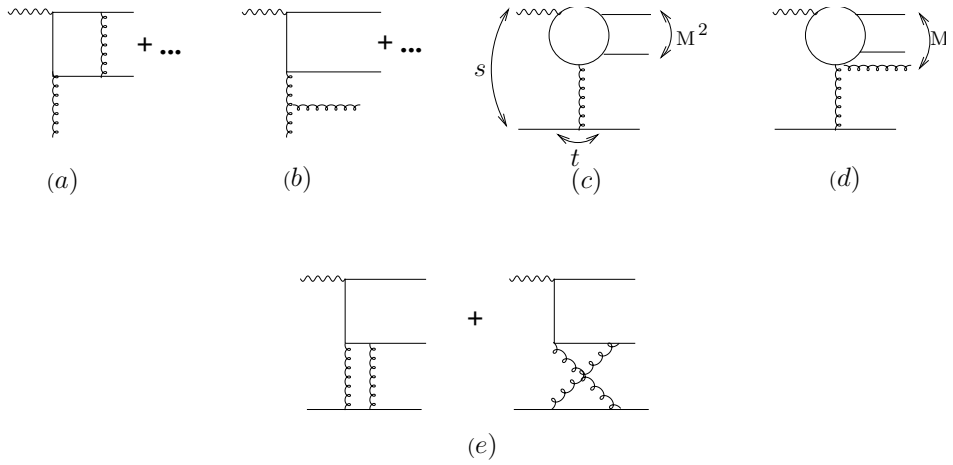

Fig. 5a–e. Schematic diagrams for next-to-leading contributions: **a** virtual corrections, **b** real corrections, **c** the process $\gamma^*+q \to (q\bar{q})+q$, **d** the process $\gamma^* + q \to (q\bar{q}g) + q$, **e** diagrams showing the reggeization of the gluon

Table 2. Table of calculations of $\mathcal{O}(\alpha_s)$ off-shell matrix elements for different types of processes

process	comments	reference
$\gamma g^* \to Q\bar{Q}$	$\|M\|^2$	[19, 35, 62]
$\gamma^* g^* \to Q\bar{Q}$	$\|M\|^2$	[35, 62]
$\gamma^* g^* \to Q\bar{Q}$	partially integrated	[63, 64]
$g^* g^* \to Q\bar{Q}$	$\|M\|^2$	[34–36]
$\gamma g^* \to J/\psi g$	$\|M\|^2$	[30, 65]
$\gamma g^* \to J/\psi g$	helicity amplitude	[66]
$\gamma^* g^* \to J/\psi g$	helicity amplitude	[66]
$g^* g^* \to J/\psi g$	helicity amplitude	[67]

NLO corrections to the process $\gamma^* g^* \to X$ contain the virtual corrections to $\gamma^* g^* \to q\bar{q}$ (Fig. 5a) and the leading order off-shell matrix element for the process $\gamma^* g^* \to q\bar{q}g$ (Fig. 5b). The calculation of the former ones has been completed, and the results for the matrix elements are published in [68]. The real corrections ($\gamma^* g^* \to q\bar{q}g$) have been obtained for helicity-summed squares of the matrix elements. For the longitudinally polarized photon they are published in [69], and results for the transversely polarized photon will be made available soon [70].

The starting point of these calculations is a study of the Regge limit of the processes $\gamma^*+q \to (q\bar{q})+q$ (Fig. 5c) and $\gamma^* + q \to (q\bar{q}g) + q$ (Fig. 5d), i.e. the contributing QCD diagrams have been calculated in the region $s = (q+p)^2 \gg Q^2,\ M^2,\ t$ and $Q^2 \gg \Lambda_{QCD}$, with $q(p)$ being the four-vector of the photon (quark). In this limit, the exchanged gluon is not an elementary but a reggeized gluon: the two gluon exchange diagrams (Fig. 5e) contain a term proportional to $\omega(t)\log(s)$, where $\omega(t)$ is the gluon Regge trajectory function. This term is not part of the subprocess $\gamma^* g^* \to q\bar{q}$ but rather belongs to the exchanged gluon. In order to find the contribution of Fig. 5e to this scattering subprocess, one first has to subtract the reggeization piece. This means that, for the subprocess $\gamma^* g^* \to q\bar{q}$, the notation '$g^*$' in NLO not only stands for 'off-shellness' but also for 'reggeized'. It also has important consequences for the factorization of the NLO off-shell subprocess inside a larger QCD diagram: the t-channel gluons connecting the different subprocesses (see, for example, $g(k_1)$ in Fig. 4) are not elementary but reggeized, and the QCD diagrams include subsets of graphs with more than two gluons in the t-channel (see Fig. 5e)

The results for the virtual corrections contain infrared singularities, both soft and virtual ones. As usual, when integrating the real corrections over the final state gluon, one finds the same infrared singularities but with opposite signs. So in the sum of virtual and real corrections one obtains an infrared finite answer. A peculiarity of this NLO calculation is the interplay with the LO process $\gamma^*+q \to (q\bar{q})+g+q$. In the latter, the process is calculated in the leading $\log(s)$ approximation (LO BFKL approximation), where the gluon has a large rapidity separation w.r.t. the $q\bar{q}$-pair (i.e. it is emitted in the central region between the $q\bar{q}$-pair and the lower quark line in Fig. 5d). As a result of this high energy (small x- or Regge) factorization, expressions for the vertex $g^* + g^* \to g$ and for the subprocess $\gamma^* g^* \to q\bar{q}$ are obtained. When turning to the NLO corrections of the process $\gamma^* + q \to (q\bar{q}g) + q$, the calculation extends to next-to-leading $\log(s)$ accuracy, but it contains, as a special case, also the LO BFKL process. In order to avoid double counting, one has to subtract the central region contribution. Only after this subtraction we have a clean separation: $q\bar{q}g$ final states without or with a large rapidity separation between the gluon and the quark-antiquark pair. The former one belongs to the NLO approximation, whereas the latter one is counted in the leading $\log(s)$ approximation.

The results for real corrections in [69] are very interesting also in the context of the QCD color dipole picture. It is well-known that the total LO $\gamma^* q$ cross section at high energies can be written in the form [71, 72]:

$$\sigma_{tot}^{\gamma^* q} = \int dz \int d\rho \left(\psi_{q\bar{q}}^{\gamma^*}(Q,z,\rho)\right)^* \sigma_{q\bar{q}}(x,z,\rho)\psi_{q\bar{q}}^{\gamma^*}(Q,z,\rho) \tag{11}$$

where z and $(1-z)$ denote the momentum fractions (w.r.t. the photon momentum q) of the quark and the antiquark, respectively, ρ is the transverse extension of the quark-antiquark pair, $\psi_{q\bar{q}}$ stands for the $q\bar{q}$ Fock component of the photon wave function, and $\sigma_{q\bar{q}}$ is the color dipole

cross section. This form of the scattering cross section is in agreement with the space time picture in the target quark rest frame: a long time before the photon reaches the target quark at rest, it splits into the quark-antiquark pair which then interacts with the target. During the interaction the transverse extension of the quark-antiquark pair remains frozen, i.e the initial quark-antiquark pair has the same ρ-value as the final one. Via the optical theorem the $\gamma^* q$ total cross section is related to the square of the scattering matrix element of the process $\gamma^* + q \to (q\bar{q}) + q$; the dipole cross section form (11) must then be a consequence of the special form of the LO amplitude for the subprocess $\gamma^* g^* \to q\bar{q}$. Since this form of the total $\gamma^* q$ cross section (which is preserved when the target quark is replaced by the target proton) looks so appealing (and also has turned out to be extremely useful in phenomenological applications), that it is desirable to investigate its validity also beyond leading order.

When trying to generalize (11) to NLO, one is led to study the square of the real corrections $\gamma^* + q \to (q\bar{q}g) + q$. If the color dipole picture remains correct (factorization in wave function and dipole cross section), this contribution naturally should lead to a new $q\bar{q}g$ Fock component of the photon wave function, and to a new interaction cross section $\sigma_{q\bar{q}g}$, which describes the interaction of the quark-antiquark-gluon system with the target quark. In [69, 70] it is shown that this is indeed the case. The form of the new photon wave function is rather lengthy (in particular for the transverse photon), and a more detailed investigation is still needed. Nevertheless, one feels tempted to conclude that the color dipole form (11) is the beginning of a general color multipole expansion, where the different Fock components of the photon wave function describe the spatial distribution of color charge inside the photon. However, before this conclusion can really be drawn, it remains to be shown that also the virtual corrections to the scattering amplitude of $\gamma^* + q \to (q\bar{q}) + q$ fit into the form (11). These corrections should lead to NLO corrections of the photon wave function or the dipole cross section. They also may slightly 'melt' the transverse extension of the quark-antiquark pair during the interaction with the target.

In summary, the results in [68–70] provide the starting point for discussing exclusive final states in the $k_\perp$-factorization scheme in NLO accuracy. However, before these formulae can be used in a numerical analysis, virtual and real corrections have to be put together, and IR finite cross sections have to be formulated. The NLO corrections to the off-shell matrix elements described in this subsection also represent the main ingredients to the NLO photon impact factor. Its importance will be discussed in Sect. 4.6.1

3.3 Gauge-invariance

The off-shell matrix elements and the cross section taken in lowest order α_s are gauge invariant, as argued in [35]. However, when extended to next order in perturbation theory, as depicted in Fig. 3, problems will occur and the off-shell matrix elements and unintegrated parton distributions are no longer necessarily gauge invariant. The following critique indicates that their definition needs further specification and that further work is needed to properly justify the formalism [73].

Basically, parton distributions are defined as a hadron expectation value of a quark and antiquark field (or two gluon fields):

$$\langle p|\bar{\psi}(y)\Gamma\psi(0)|p\rangle, \tag{12}$$

with an appropriate Fourier transformation on the space-time argument y^μ, some appropriate Dirac matrix Γ and some appropriate normalization. This definition is not gauge invariant, so one must either specify the gauge or one modifies the definition to make it gauge invariant:

$$\langle p|\bar{\psi}(y)\Gamma P e^{-ig\int_0^y dy'^\mu A_\mu^\alpha(y')t_\alpha}\psi(0)|p\rangle. \tag{13}$$

Here, t_α are generating matrices for the $SU(3)$ color group of QCD, and the symbol P denotes that the gluon fields are laid out in their order on the path in the integral from 0 to y.

The big question is which path is to be used. For the integrated parton distributions, y is at a light-like separation from 0: normally $y^- \neq 0$, $y^+ = y_\perp = 0$, and then taking the path along the light-like straight line joining 0 and $y = (0, y^-, 0_\perp)$ is natural and correct. But for unintegrated distributions, this is not so simple; one has a choice of paths. The choice is not arbitrary but is determined by the derivation: i.e., the definition is whatever is appropriate to make a correct factorization theorem.

This can be seen from the analysis of gluon emission that we have already described. This analysis is only applicable if ladder diagrams, as in Fig. 3, actually dominate. In fact, in a general gauge, non-ladder diagrams are as important as ladder diagrams. This is the case, for example, in the Feynman gauge. The standard leading-logarithm analysis suggests, as is commonly asserted, that the appropriate gauge is a light-cone gauge $n \cdot A = 0$, where n is a light-like vector in a suitable direction, for then non-ladder contributions are suppressed in the LLA analysis. From this one would conclude that the off-shell matrix elements and the unintegrated parton distributions are defined as the appropriate field theory Green functions in light-cone gauge.

Closer examination shows that there must be problems since the unintegrated parton distributions are divergent. This was shown quite generally by Collins and Soper [74, 75] as part of their derivation of factorization for transverse-momentum distributions. They found they needed to derive factorization and to define unintegrated parton distributions in a *non*-light-like axial gauge, i.e., with $n^2 \neq 0$ [1]. They derived an evolution equation for the dependence on the gauge-fixing vector; the evolution is quite important and contains doubly-logarithmic Sudakov effects. In the limit $n^2 \to 0$, the parton distributions become so singular that they are not defined. The divergences are associated with the emission of gluons of

[1] An equivalent and probably better definition can be made with suitable path-ordered exponential in the operator

arbitrarily negative rapidity with respect to the parent hadron; commonly these are called soft gluons, and a non-light-like gauge-fixing vector provides a cutoff on the divergences. It is normally said that soft gluons cancel in QCD cross sections. However, the standard cancellation requires an integral over all parton transverse momentum, which is of course not applicable in an unintegrated parton density.

The divergences can readily be seen in one-loop graphs, and are a generalization of divergences known to occur in light-cone gauge. Modification of the $i\epsilon$ prescription of the $1/k\cdot n$ singularity of the gluon propagator, as is commonly advocated, is not sufficient, since this does not remove the divergence in the emission of *real* gluons, for which the singularity is an endpoint singularity in $k \cdot n$.

Clearly, in all the derivations of the BFKL and related equations, there must be an appropriate cutoff. Unfortunately, this is not normally made very explicit, even though an explicit specification of the cutoff is vitally important if the formalism is to make sense beyond LO. One can expect, that such a cutoff is a cutoff in angle or rapidity, and it should be related to angular ordering, supporting the intuitive approximate picture. However, the presence of the cutoff implies that there is an extra parameter in the parton distributions, whose variation should be understood. Balitsky [76] has worked in this direction, although his formulation does not appear to have developed far enough to address the issues in the present document.

A proper derivation will also result in an explicit definition of a reggeized gluon. Such a definition is not readily extracted from the original BFKL publications. At most these publications provide a definition as a property of a solution of their equation. No explicit definition is given whereby quantities involving reggeized gluons are matrix elements of some operator or other.

4 Unintegrated parton distributions

4.1 Introduction

The conventional parton distributions describe the density of partons carrying a certain longitudinal momentum fraction inside the proton. These distributions are integrated over the transverse momenta of the partons up to the factorization scale μ. However, in order to describe some exclusive processes it becomes necessary to consider the transverse momenta of the partons and thus use so called unintegrated gluon distributions $\mathcal{A}(x,k_\perp^2,\mu^2)$. Unintegrated parton distributions account for the resummation of a variety of logarithmically enhanced terms, such as

$$\begin{aligned}&\left(\alpha_s \log(\mu^2/\Lambda^2)\right)^n,\\ &\left(\alpha_s \log(\mu^2/\Lambda^2)\log(1/x)\right)^n,\\ &\left(\alpha_s \log(1/x)\right)^n \quad \text{and} \quad \left(\alpha_s \log^2(\mu^2/k_\perp^2)\right)^n\end{aligned} \tag{14}$$

The unintegrated parton distributions describe the probability of finding a parton carrying a longitudinal momentum fraction x and a transverse momentum $k_\perp$ at the factorization scale μ. The unintegrated gluon density $x\mathcal{A}(x,k_\perp^2,\mu^2)$ can be related to the integrated one $xg(x,\mu^2)$ by:

$$xg(x,\mu^2) \simeq \int_0^{\mu^2} dk_\perp^2 x\mathcal{A}(x,k_\perp^2,\mu^2)\,. \tag{15}$$

The $\simeq$ sign in the above equation indicates, that there is no strict equality between unintegrated and integrated parton distributions, as neither are observables.

In unintegrated parton distributions, the contribution from the large logarithms in x and μ^2, the terms specified above in expression (14), can be correctly disentangled. However, the unintegrated parton distributions are defined only as a functions of three variables x, $k_\perp^2$, μ^2. The 4-vector k of the propagator gluon in initial state cascade is given by:

$$k = (k^+, k^-, k_\perp)$$

with $k^+ = x^+P^+$, $k^- = x^-P^-$. The virtuality k^2 is:

$$k^2 = k^+k^- - k_\perp^2 = x^+x^-P^-P^+ - k_\perp^2.$$

In the region of strongly ordered k^+, the typical values of k^- are small enough that it can be neglected in the hard scattering factor. For example, the virtuality is dominated by the transverse momentum only:

$$k^2 \simeq -k_\perp^2.$$

However, the k^- integral is still present, and in fact, part of the definition of an unintegrated parton density is, that the relevant matrix element of a gluonic operator is integrated over all k^-. This is the reason, why only $x = x^+$ is kept in the unintegrated gluon density.

The all-loop resummation of the $\alpha_s \log 1/x$ contribution at small x leads to *Reggeization* of the gluon vertex, giving rise to a significant form factor. The *Regge* form factor Δ_{Regge}, often also called *non-Sudakov* form factor Δ_{ns}, regularizes the $1/z$ divergence in the splitting function,

$$P_g(z_+) \propto \frac{\Delta_{\text{Regge}}(k_\perp, z_+)}{z_+}. \tag{17}$$

The Δ_{Regge} of BFKL is given by [77]:

$$\begin{aligned}&\Delta_{\text{Regge}}(z_+, k_\perp^2)\\ &= \exp\left(-\bar{\alpha}_{\text{S}} \int_{z_+}^1 \frac{dz'}{z'} \int \frac{dq_\perp^{'2}}{q_\perp^{'2}} \Theta(k_\perp^2 - q_\perp^{'2})\Theta(q_\perp^{'2} - q_0^2)\right)\end{aligned} \tag{18}$$

with $\bar{\alpha}_{\text{S}} = \frac{C_A\alpha_s}{\pi} = \frac{3\alpha_s}{\pi}$ and q_0 being a lower cutoff. This form factor can be expanded by a power series and then symbolically represented as in Eq. (18) (on top of the next page) where the small x resummation of the virtual corrections becomes obvious. Such a diagrammatic representation is of course gauge dependent. It should be noted that the Regge form factor in this way looks like the Sudakov form factor [78, 79] used to regularize the $1/(1-z)$ pole in standard DGLAP evolution, but the resummed diagrams

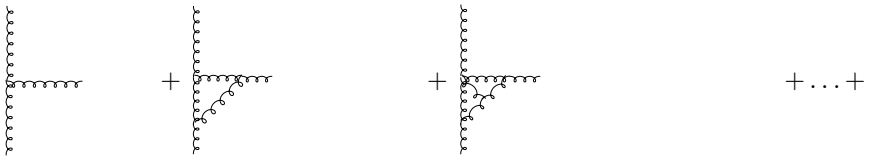

$$\bar{\alpha}_{\rm S}(k_\perp)\frac{1}{z_+}\left[1+\bar{\alpha}_{\rm S}\log(z)\log\left(\frac{k_\perp^2}{q_0^2}\right)+\left(\frac{1}{2!}\bar{\alpha}_{\rm S}\log(z)\log\left(\frac{k_\perp^2}{q_0^2}\right)\right)^2 \quad \dots\right] \tag{18}$$

involve small z rather than large ones. This similarity is used in the derivation of the Linked Dipole Chain model below.

In interpreting the results quoted in this section, the reader should bear in mind the caveats explained in Sec. 3.3, that as yet, no fully explicit definition of the parton distributions has been given.

4.2 The CCFM evolution

According to the CCFM [41–44] evolution equation the emission of gluons during the initial cascade is only allowed in an angular-ordered region of phase space. The maximum allowed angle Ξ is defined by the hard scattering quark box, producing the (heavy) quark pair. In terms of Sudakov variables the quark pair momentum is written as:

$$p_q + p_{\bar{q}} = \Upsilon(P_1 + \Xi P_2) + \vec{Q}_\perp \tag{19}$$

where Υ ($\Upsilon\Xi$) is the positive (negative) light-cone momentum fraction of the quark pair, $P_{1,2}$ are the four-vectors of incoming beam particles, respectively and $\vec{Q}_t$ is the vectorial sum of the transverse momenta of the quark pair in the laboratory frame. Similarly, the momenta p_i of the gluons emitted during the initial state cascade are given by (here treated massless):

$$p_i = \upsilon_i(P_1 + \xi_i P_2) + p_{\perp i}\ , \quad \xi_i = \frac{p_{\perp i}^2}{s\upsilon_i^2}, \tag{20}$$

with $\upsilon_i = (1-z_i)x_{i-1}$, $x_i = z_i x_{i-1}$ and $s = (P_1+P_2)^2$ being the squared center of mass energy. The variable ξ_i is connected to the angle of the emitted gluon with respect to the incoming proton and x_i and υ_i are the momentum fractions of the exchanged and emitted gluons, while z_i is the ratio of the energy fractions in the branching $(i-1) \to i$ and $p_{\perp i}$ is the transverse momentum of the emitted gluon i.

The angular-ordered region is then specified by (Fig. 2):

$$\xi_0 < \xi_1 < \cdots < \xi_n < \Xi \tag{21}$$

which becomes:

$$z_{i-1}\bar{q}_{i-1} < \bar{q}_i \tag{22}$$

where the rescaled transverse momenta $\bar{q}_i$ of the emitted gluons is defined by:

$$\bar{q}_i = x_{i-1}\sqrt{s\xi_i} = \frac{p_{\perp i}}{1-z_i}\ . \tag{23}$$

It is interesting to note, that the angular ordering constraint, as given by (22), reduces to ordering in transverse momenta $p_\perp$ for large z, whereas for $z \to 0$, the transverse momenta are free to perform a so-called random walk.

The CCFM evolution equation with respect to the scale $\bar{q}^2$ can be written in a differential form [44]:

$$\begin{aligned}&\bar{q}^2\frac{d}{d\bar{q}^2}\frac{x\mathcal{A}\left(x,k_\perp^2,\bar{q}^2\right)}{\Delta_s(\bar{q}^2,Q_0^2)} \\ &= \int dz\frac{d\phi}{2\pi}\frac{\tilde{P}\left(z,(\bar{q}/z)^2,k_\perp^2\right)}{\Delta_s(\bar{q}^2,Q_0^2)}\,x'\mathcal{A}\left(x',k_\perp'^2,(\bar{q}/z)^2\right)\end{aligned} \tag{24}$$

where $\mathcal{A}(x,k_\perp^2,\bar{q}^2)$ is the unintegrated gluon density, depending on x, $k_\perp^2$ and the evolution variable $\mu^2 = \bar{q}^2$. The splitting variable is $z = x/x'$ and $\vec{k_\perp}' = (1-z)/z\vec{q} + \vec{k_\perp}$, where the vector $\vec{q}$ is at an azimuthal angle ϕ. The Sudakov form factor Δ_s is given by:

$$\begin{aligned}&\Delta_s(\bar{q}^2,Q_0^2) \\ &= \exp\left(-\int_{Q_0^2}^{\bar{q}^2}\frac{dq^2}{q^2}\int_0^{1-Q_0/q}dz\frac{\bar{\alpha}_{\rm S}\left(q^2(1-z)^2\right)}{1-z}\right)\end{aligned} \tag{25}$$

with $\bar{\alpha}_{\rm S} = \frac{C_A\alpha_s}{\pi} = \frac{3\alpha_s}{\pi}$. For inclusive quantities at leading-logarithmic order the Sudakov form factor cancels against the $1/(1-z)$ collinear singularity of the splitting function.

The splitting function $\tilde{P}$ for branching i is given by:

$$\begin{aligned}\tilde{P}_g(z_i,q_i^2,k_{\perp i}^2) = &\frac{\bar{\alpha}_{\rm S}(q_i^2(1-z_i)^2)}{1-z_i} \\ &+\frac{\bar{\alpha}_{\rm S}(k_{\perp i}^2)}{z_i}\Delta_{ns}(z_i,q_i^2,k_{\perp i}^2)\end{aligned} \tag{26}$$

where the non-Sudakov form factor Δ_{ns} is defined as:

$$\begin{aligned}&\log\Delta_{ns}(z_i,q_i^2,k_{\perp i}^2) \\ &= -\bar{\alpha}_{\rm S}\int_{z_i}^1\frac{dz'}{z'}\int\frac{dq^2}{q^2}\Theta(k_{\perp i}-q)\Theta(q-z'q_i)\ .\end{aligned} \tag{27}$$

The upper limit of the z' integral is constrained by the Θ functions in (27) by: $z_i \le z' \le \min(1, k_{\perp i}/q_i)$, which results in the following form of the non-Sudakov form factor [80]:

$$\log\Delta_{ns} = -\bar{\alpha}_{\rm S}(k_{\perp i}^2)\log\left(\frac{z_0}{z_i}\right)\log\left(\frac{k_{\perp i}^2}{z_0 z_i q_i^2}\right) \tag{28}$$

where

$$z_0 = \begin{cases} 1 & \text{if} k_{\perp i}/q_i > 1 \\ k_{\perp i}/p_{\perp i} & \text{if} z_i < k_{\perp i}/q_i \leq 1 \\ z_i & \text{if} k_{\perp i}/q_i \leq z_i \end{cases} .$$

The unintegrated gluon density $\mathcal{A}(x, k_\perp^2, \bar{q}^2)$ is a function also of the angular variable $\bar{q}$, ultimately limited by an angle, $\bar{q}^2 = x_{n-1}^2 \Xi s$, defined by the hard interaction, and the two scales $k_\perp^2, \bar{q}^2$ in $\mathcal{A}(x, k_\perp^2, \bar{q}^2)$ should not come as a surprise. As we are concentrating on an evolution, which is not ordered in transverse momenta, it is natural to have more than one scale in the problem. The typical example of such a two scale evolution process is $\gamma^*\gamma^* \to$ hadrons scattering where the photons are highly virtual, but the virtualities still being much smaller than the total energy, $s \gg Q_1^2 \approx Q_2^2 \gg \Lambda_{\rm QCD}$. Another example is DIS with a forward high-$p_\perp$ jet, where Q^2 and $p_\perp^2$ provide the scales. In the DGLAP approximation the evolution is performed between a small and a large scale – a large scale probe resolves a target at a smaller scale. It is obvious, that this evolution is not appropriate for the case of two similar scales and instead an evolution in rapidity, or angle, is needed.

In CCFM the scale $\bar{q}$ (coming from the maximum angle) can be related to the evolution scale in the collinear parton distributions. This becomes obvious since

$$\bar{q}^2 \sim x_g^2 \Xi s = y x_g s = \hat{s} + Q_\perp^2 . \tag{29}$$

The last expression is derived by using $p_q + p_{\bar{q}} \simeq x_g P_2 + y P_1 + \vec{Q}_\perp$, $\Xi \simeq y/x_g$ and $\hat{s} = y x_g s - Q_\perp^2$. This can be compared to a possible choice of the renormalization and factorization scale μ^2 in the collinear approach with $\mu^2 = Q_\perp^2 + 4 \cdot m_q^2$ and the similarity between μ and $\bar{q}$ becomes obvious.

4.3 LDC and the transition between BFKL and DGLAP

The Linked Dipole Chain (LDC) model [50, 51] is a reformulation of CCFM which makes the evolution explicitly left–right symmetric, which will be discussed in Sect. 4.6 in more detail. LDC relies on the observation that the non-Sudakov form factor in (27), despite its name, can be interpreted as a kind of Sudakov form factor giving the no-emission probability in the region of integration. To do this an additional constraint on the initial-state radiation is added requiring the transverse momentum of the emitted gluon to be above the smaller of the transverse momenta of the connecting propagating gluons:

$$p_{\perp i}^2 > \min(k_{\perp i-1}^2, k_{\perp i}^2). \tag{30}$$

Emissions failing this cut will instead be treated as final-state emissions and need to be resummed in order not to change the total cross section. In the limit of small z and imposing the kinematic constraint of (65) (see Sect. 4.6 for further details) gives a factor which if it is multiplied with each emission, completely cancels the non-Sudakov and thus, in a sense *de-reggeizes* the gluon.

One may ask when it is appropriate to use collinear factorization (DGLAP) and when we must account for effects of BFKL and $k_\perp$-factorization. Clearly, when $k_\perp$ is large and $1/x$ is limited we are in the DGLAP regime, and when $1/x$ is large and $k_\perp$ is limited we are in the BFKL regime. An essential question is then: What is large? Where is the boundary between the regimes, and what is the behavior in the transition region? Due to the relative simplicity of the LDC model, which interpolates smoothly between the regimes of large and small $k_\perp$, it is possible to give an intuitive picture of the transition. In the following x is always kept small, and leading terms in $\log 1/x$ are studied. Thus the limit for large $k_\perp$ does not really correspond to the DGLAP regime, but more correctly to the double-log approximation.

First we will discuss the case of a fixed coupling. For large values of $k_\perp$ (in the "DGLAP region") the unintegrated structure function $\mathcal{F}(x, k_\perp^2)$ is dominated by contributions from chains of gluon propagators which are ordered in $k_\perp$. The result is a product of factors $\bar{\alpha}_{\rm S} \cdot \frac{dx_i}{x_i} \cdot \frac{dk_{\perp i}^2}{k_{\perp i}^2}$ [1–4]:

$$\mathcal{F}(x, k_\perp^2) \sim \sum_N \int \prod^N \bar{\alpha}_{\rm S}\, dl_i \theta(l_{i+1} - l_i)\, d\kappa_i \Theta(\kappa_{i+1} - \kappa_i)$$

where

$$\bar{\alpha}_{\rm S} \equiv \frac{3\alpha_s}{\pi},\ l \equiv \log(1/x) \text{ and } \kappa \equiv \log(k_\perp^2/\Lambda^2) . \tag{31}$$

Integration over κ_i with the Θ-functions gives the phase space for N ordered values κ_i. The result is $\kappa^N/N!$. The integrations over l_i give a similar result, and thus we obtain the well-known double-log result

$$\mathcal{F}(x, k_\perp^2) \sim \sum_N \bar{\alpha}^N \cdot \frac{l^N}{N!} \cdot \frac{\kappa^N}{N!} = I_0(2\sqrt{\bar{\alpha} l \kappa}) . \tag{32}$$

In the BFKL region also non-ordered chains contribute, and the result is a power-like increase $\sim x^{-\lambda}$ for small x-values [5–7].

The CCFM [41–44] and the LDC model [50, 51, 81] interpolate between the DGLAP and BFKL regimes. In the LDC model the possibility to "go down" in $k_\perp$, from κ' to a smaller value κ, is suppressed by a factor $\exp(\kappa - \kappa')$. The effective allowed distance for downward steps is therefore limited to about one unit in κ. If this quantity is called δ, the result is, that the phase space factor $\frac{\kappa^N}{N!}$ is replaced by $\frac{(\kappa + N\delta)^N}{N!}$. Thus we obtain:

$$\mathcal{F}(x, k_\perp^2) \sim \sum_N \frac{(\bar{\alpha} l)^N}{N!} \frac{(\kappa + N\delta)^N}{N!} . \tag{33}$$

When κ is very large, this expression approaches (32). When κ is small we find, using Sterling's formula, that $\mathcal{F}(x, k_\perp^2) \sim \sum_N (\bar{\alpha}_{\rm S} l \delta e)^N / N! = \exp(\lambda l) \equiv x^{-\lambda}$, with $\lambda =$

$\bar{\alpha}_S \delta e$. For $\delta = 1$ this gives $\lambda = e\bar{\alpha}_S = 2.72\bar{\alpha}_S$, which is very close to the leading order result for the BFKL equation, $\lambda = 4 \log 2\, \bar{\alpha}_S = 2.77\bar{\alpha}_S$. Thus (33) interpolates smoothly between the DGLAP and BFKL regimes. It is also possible to see that the transition occurs for a fixed ratio between κ and l, $\kappa/l \approx e\bar{\alpha}_S$.

For a running coupling a factor $\bar{\alpha}_S\, d\kappa$ in (31) is replaced by $\alpha_0\, d\kappa/\kappa = \alpha_0\, du$, where $\alpha_0 \equiv \bar{\alpha}_S \kappa$, $u \equiv \log(\kappa/\kappa_0)$ and κ_0 is a cutoff. In the large $k_\perp$ region (the "DGLAP region") the result is therefore similar to (32), but with $\bar{\alpha}_S \kappa$ replaced by $\alpha_0 u$. For small x-values we note that the allowed effective size of downward steps, which is still one unit in κ, is a sizeable interval in u for small κ, but a very small interval in u for larger κ.

This is the reason for an earlier experience [51], which showed that a typical chain contains two parts. In the first part the $k_\perp$-values are relatively small, and it is therefore easy to go up and down in $k_\perp$, and non-ordered $k_\perp$-values are important. The second part is an ordered (DGLAP-type) chain, where $k_\perp$ increases towards its final value.

Let us study a chain with N links, out of which the first $N - k$ links correspond to the first part with small non-ordered $k_\perp$ values, and the remaining k links belong to the second part with increasing $k_\perp$. Assume that the effective phase space for each u_i in the soft part is given by a quantity Δ. Then the total weight for this part becomes Δ^{N-k}. For the k links in the second, ordered, part the phase space becomes as in the DGLAP case $u^k/k!$. Thus the total result is ($G \equiv \kappa \mathcal{F}$)

$$
\begin{aligned}
G &\sim \sum_N \frac{(\alpha_0 l)^N}{N!} \sum_{k=0}^{N} \frac{u^k}{k!} \Delta^{N-k} \\
&= \sum_N \frac{(\alpha_0 l \Delta)^N}{N!} \sum_{k=0}^{N} \frac{(u/\Delta)^k}{k!}\,. \qquad (34)
\end{aligned}
$$

This simple model also interpolates smoothly between the DGLAP and BFKL regions. For large u-values the last term in the sum over k dominates, which gives the "DGLAP" result

$$
\begin{aligned}
G &\sim \sum (\alpha_0 l u)^N/(N!)^2 \\
&= I_0(2\sqrt{\alpha_0 l u}) \\
&\approx (16\pi^2 \alpha_0 l u)^{-1/4} \cdot \exp(2\sqrt{\alpha_0 l u}). \qquad (35)
\end{aligned}
$$

For small u-values the sum over k gives approximately $\exp(u/\Delta)$, and thus

$$
G \sim \exp(\alpha_0 \Delta l) \cdot \exp(u/\Delta) = x^{-\lambda} \kappa^{\alpha_0/\lambda}, \text{ with } \lambda = \alpha_0 \Delta. \qquad (36)
$$

The transition between the regimes occurs now for a fixed ratio between $u/l \approx \lambda^2/\alpha_0$, which is of order 0.1 if λ is around 0.3. The result is illustrated in Fig. 6, which shows how the expression in (34) interpolates between the DGLAP and BFKL limits in (35) and (36) for large and small $k_\perp$ [2].

[2] In the framework of $N = 4$ SUSY, where the corresponding coupling is not running, the relations between DGLAP and BFKL equations has been found in [82–85] for the first two orders of perturbation theory. These results can be useful for possible future study of the corresponding approximate relations in QCD

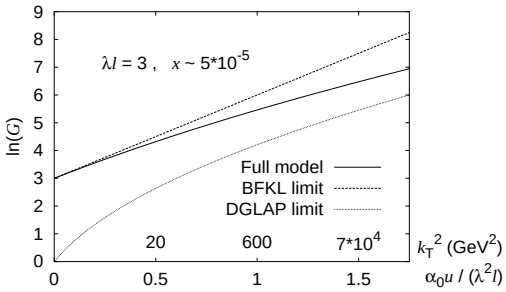

Fig. 6. Results for a running coupling for $\lambda l = 3$, which for $\lambda = 0.3$ means $x = 5 \cdot 10^{-5}$. (Note that this x-value corresponds only to the chain between the "observed" low energy gluon and the parent soft gluon.) The solid line corresponds to the model in (34), the dashed line to the BFKL limit, (36), and the dotted line to the DGLAP limit in (35). The abscissa is the variable $w = \alpha_0 u/\lambda^2 l$ defined so that the transition occurs for $w \approx 1$. The corresponding values for $k_\perp^2$ in GeV^2 for $\lambda = 0.3$ and $\lambda l = 3$ are also indicated

The simple models in (33) and (34), for fixed and running couplings respectively, interpolate smoothly between large and small $k_\perp$-values. They contain the essential features of the CCFM and LDC models, and can therefore give an intuitive picture of the transition between these two regimes. The transition occurs for a fixed ratio between $\log k_\perp^2$ and $\log 1/x$ for fixed coupling, and between $\log(\log k_\perp^2)$ and $\log 1/x$ for a running coupling. A more extensive discussion, including effects of non-leading terms in $\log 1/x$ and the properties of Laplace transforms, is found in [86].

4.4 The CCFM equation in the transverse coordinate representation

It might be useful to consider the CCFM equation using the transverse coordinate (or impact parameter) [87] b conjugate to the transverse momentum $k_\perp$ and to introduce the b dependent gluon distribution $\bar{\mathcal{A}}(x, b, \bar{q}^2)$ defined by the Fourier-Bessel transform of $\mathcal{A}(x, k_\perp^2, \bar{q}^2)$:

$$
\bar{\mathcal{A}}(x, b, \bar{q}^2) = \int_0^\infty k_\perp dk_\perp J_0(b k_\perp) \mathcal{A}(x, k_\perp^2, \bar{q}^2). \qquad (37)
$$

where $J_0(u)$ is the Bessel function. The advantage of this representation becomes particularly evident in the so called 'single -loop' approximation that corresponds to the replacement $\bar{q}/z \to \bar{q}$ and $\Delta_{NS} \to 1$. In this approximation the CCFM equation reduces to the conventional DGLAP evolution and (24) is diagonalized by the Fourier - Bessel transformation provided that we set the same argument $\mu^2 \sim \bar{q}^2$ in both terms in this equation. The evolution equation for $\bar{\mathcal{A}}(x, b, \bar{q}^2)$ reads:

$$\bar{q}^2 \frac{d}{d\bar{q}^2} \frac{x\bar{\mathcal{A}}(x,b,\bar{q}^2)}{\bar{\Delta}_s(\bar{q}^2,Q_0^2)} = \bar{\alpha}_S(\bar{q}^2) \int dz \bar{P}(z) J_0[(1-z)\bar{q}b] \frac{x'\bar{\mathcal{A}}(x',b,\bar{q}^2)}{\bar{\Delta}_s(\bar{q}^2,Q_0^2)} \quad (38)$$

where

$$\bar{P}(z) = \frac{1}{1-z} - 2 + z(1-z) + \frac{1}{z} . \quad (39)$$

In (38) the argument μ^2 of the QCD coupling was set $\mu^2 = \bar{q}^2$ and

$$\bar{\Delta}_s(\bar{q}^2,Q_0^2) = \exp\left(- \int_{Q_0^2}^{\bar{q}^2} \frac{dq^2}{q^2} \int_0^{1-Q_0/q} dz \bar{\alpha}_S(q^2) z \bar{P}(z) \right) \quad (40)$$

In the splitting function $\bar{P}(z)$ we have included the terms which are non-singular at $z = 0$ or $z = 1$ in order to get a complete DGLAP evolution equation for the integrated gluon distribution. For the same reason we have also extended the definition of the Sudakov form factor by including the complete splitting function $\bar{P}(z)$ and not only its part which is singular at $z = 1$ (cf. (40)).

Equation (38) can be solved exactly after going to the moment space and introducing the moment function $\tilde{\mathcal{A}}_\omega(b,\bar{q}^2)$ defined by:

$$\tilde{\mathcal{A}}_\omega(b,\bar{q}^2) = \int_0^1 dx x^\omega \bar{\mathcal{A}}(x,b,\bar{q}^2) . \quad (41)$$

The solution of the evolution equation for the moment function $\tilde{\mathcal{A}}_\omega(b,\bar{q}^2)$ reads:

$$\tilde{\mathcal{A}}_\omega(b,\bar{q}^2) = \tilde{\mathcal{A}}^0_\omega(b) \cdot \exp\left[\int_{Q_0^2}^{\bar{q}^2} \frac{dq^2}{q^2} \bar{\alpha}_S(q^2) \times \int_0^{1-Q_0/\bar{q}} dz z \bar{P}(z) (z^{\omega-1} J_0(bq(1-z)) - 1) \right] \quad (42)$$

where $\tilde{\mathcal{A}}^0_\omega(b)$ is the Fourier-Bessel transform of the (input) unintegrated distribution at $\bar{q} = Q_0$. It should be noted that at $b = 0$, $\tilde{\mathcal{A}}_\omega(b,\bar{q}^2)$ is proportional to the moment function of the integrated gluon distribution $g(x,\bar{q})$. The solution (42) at $b = 0$ reduces to the solution of the LO DGLAP equation for the moment function of the integrated gluon distribution. It should also be noted that the integrand in (42) is free from singularities at $z = 1$ and so we can set $Q_0 = 0$ in the upper integration limit over dz. The formalism presented above is similar to that used for the description of the transverse momentum distributions in (for instance) the Drell-Yan process (see e.g. [88–91]). In order to obtain more insight into the structure of the unintegrated distribution which follows from the CCFM equation in the single loop approximation it is useful to adopt in (37) the following approximation of the Bessel function:

$$J_0(u) \simeq \Theta(1-u) \quad (43)$$

which gives:

$$\mathcal{A}(x,k_\perp^2,\bar{q}^2) \simeq 2 \frac{d\bar{\mathcal{A}}(x,b=1/k_\perp,\bar{q}^2)}{dk_\perp^2} . \quad (44)$$

Using the same approximation for the Bessel function in (42) we get, after some rearrangements, the following relation between unintegrated and integrated gluon distributions:

$$\mathcal{A}(x,k_\perp^2,\bar{q}^2) \simeq \frac{d}{dk_\perp^2}[g(x,k_\perp^2)\bar{\Delta}_s(\bar{q}^2,k_\perp^2)] \quad (45)$$

Similar relation has also been used in [92, 93] (see also (55) in the next section).

In the general 'all loop' case, the non-Sudakov form-factor generates contributions which are no longer diagonal in the b space and so the merit of using this representation is less apparent. However in the leading $\log(1/x)$ approximation at small x the CCFM equation reduces to the BFKL equation with no scale dependence and the kernel of the BFKL equation in b space is the same as that in the (transverse) momentum space. The work to explore the CCFM equation in b space beyond the 'single loop' and BFKL approximations is in progress.

4.5 Available parameterizations of unintegrated gluon distributions

Depending on the approximations used, different unintegrated gluon distributions can be obtained (see (15)). Here we describe some of the so far published ones and make some comparisons[3]. We use the following classification scheme: $x\mathcal{G}(x,k_\perp^2)$ describes DGLAP type unintegrated gluon distributions, $x\mathcal{F}(x,k_\perp^2)$ is used for pure BFKL and $x\mathcal{A}(x,k_\perp^2,\bar{q}^2)$ stands for a CCFM type or any other type having two scales involved.

Derivative of the integrated gluon density

Ignoring the fact that the unintegrated density may depend on two scales we can invert (15) which gives the unintegrated gluon density $\mathcal{G}(x,k_\perp^2)$:

$$x\mathcal{G}(x,k_\perp^2) = \left. \frac{dxg(x,\mu^2)}{d\mu^2} \right|_{\mu^2=k_\perp^2} . \quad (46)$$

Here $xg(x,\mu^2)$ can be any of the parameterizations of the gluon density available.

GBW (Golec-Biernat Wüsthoff [94])

Within the color-dipole approach of [94, 95], a simple parameterization of the unintegrated gluon density was obtained which successfully describes both inclusive and also diffractive scattering. The unintegrated gluon density is given by [94]:

$$\mathcal{F}(x,k_\perp^2) = \frac{3\sigma_0}{4\pi^2\alpha_s} R_0^2(x) k_\perp^2 \exp\left(-R_0^2(x)k_\perp^2\right) \quad (47)$$

[3] Parameterizations of the unintegrated gluon distributions described here are available as a FORTRAN code from `http://www.thep.lu.se/Smallx`

with $\sigma_0 = 29.12$ mb, $\alpha_s = 0.2$ and

$$R_0(x) = \frac{1}{Q_0}\left(\frac{x}{x_0}\right)^{\lambda/2}$$

and $Q_0 = 1$ GeV, $\lambda = 0.277$ and $x_0 = 0.41 \cdot 10^{-4}$, where the parameters correspond to the parameterization which includes charm [95].

RS (Ryskin, Shabelski [96])

A parameterization of the unintegrated gluon density satisfying the BFKL equation but including also the non-singular parts of the gluon splitting function as given by DGLAP is presented in [96]. The integrated gluon density $xg(x,\mu^2)$ is defined by:

$$xg(x,\mu^2) = \frac{1}{4\sqrt{2}\pi^3}\int_0^{\mu^2}\phi(x,k_\perp^2)dk_\perp^2\ . \tag{48}$$

The function $\phi(x,k_\perp^2)$ is obtained by a solution of the evolution equation (including LO BFKL and the remaining part of the DGLAP splitting function, but without applying the *kinematic constraint*) in the perturbative region $k_\perp^2 > Q_0^2$. The non-perturbative part of the gluon density is identified as the collinear gluon density $xg(x,Q_0^2)$ at a small scale $Q_0^2 \sim 4$ GeV^2:

$$\mathcal{F}(x,k_\perp^2) = \begin{cases} \frac{xg(x,Q_0^2)}{Q_0^2} & \text{if } k_\perp^2 < Q_0^2 \\ \frac{\phi(x,k_\perp^2)}{4\sqrt{2}\pi^3} & \text{if } k_\perp^2 \geq Q_0^2 \end{cases}\ . \tag{49}$$

An explicit form of the parameterization of the function ϕ together with the fitted parameters are given in [96].

KMS (Kwiecinski, Martin, Stasto [97])

In the approach of *KMS* [97] three modifications to the BFKL equation are introduced in order to extend its validity to cover the full range in x. Firstly, a term describing the leading order DGLAP evolution is added. The inclusion of this term has the effect of softening the small x rise and to change the overall normalization. Secondly, the kinematic constraint (65) is applied, which has its origin in the requirement that the virtuality of the exchanged gluon is dominated by its transverse momentum. Thirdly, the BFKL equation is solved only in the region of $k_\perp > k_{\perp 0}$, whereas the non-perturbative region is provided by the collinear gluon density $xg(x,k_{\perp 0}^2)$ at the scale $k_{\perp 0}$. The border between the perturbative and non-perturbative regions has been taken to be $k_{\perp 0} = 1$ GeV^2.

Also a term which allows the quarks to contribute to the evolution of the gluon has been introduced. The single quark contribution is controlled through the $g \to q\bar{q}$ splitting. The input gluon and quark distributions to this *unified* DGLAP-BFKL evolution equation are determined by a fit to HERA F_2 data. The unintegrated gluon density $\mathcal{F}(x,k_\perp^2)$ is still only a function of x and $k_\perp^2$, which strictly satisfies:

$$\begin{aligned} xg(x,Q^2) &= \int^{Q^2}\frac{dk_\perp^2}{k_\perp^2}f(x,k_\perp^2) \\ &= \int^{Q^2} dk_\perp^2\,\mathcal{F}(x,k_\perp^2). \end{aligned} \tag{50}$$

JB (J. Blümlein [98])

In the approach of *JB* [98] the general $k_\perp$-factorization formula:

$$\sigma(x,\mu^2) = \int dk_\perp^2\,\hat{\sigma}(x,k_\perp^2,\mu^2)\otimes\mathcal{A}(x,k_\perp^2,\mu^2)$$

is rewritten in the form [36]:

$$\begin{aligned} &\sigma(x,\mu^2) = \sigma^0(x,\mu^2)\otimes g(x,\mu^2) \\ &+\int_0^\infty dk_\perp^2\left(\hat{\sigma}\left(x,k_\perp^2,\mu^2\right)-\sigma^0\left(x,\mu^2\right)\right)\otimes\mathcal{A}\left(x,k_\perp^2,\mu^2\right), \end{aligned} \tag{51}$$

which gives the relation:

$$g(x,\mu^2) = \int_0^\infty dk_\perp^2\,\mathcal{A}(x,k_\perp^2,\mu^2).$$

In the case of (51) the $k_\perp$ dependent gluon distribution satisfying the BFKL equation can be represented as the convolution of the integrated gluon density $xg(x,\mu^2)$ (for example GRV [99]) and a universal function $\mathcal{B}(x,k_\perp^2,\mu^2)$:

$$\mathcal{A}(x,k_\perp^2,\mu^2) = \int_x^1 \mathcal{B}(z,k_\perp^2,\mu^2)\,\frac{x}{z}\,g(\frac{x}{z},\mu^2)\,dz\ . \tag{52}$$

The universal function $\mathcal{B}(x,k_\perp^2,\mu^2)$ can be represented as a series (see [98]):

$$\sum_{i=1}^{N=\infty} d_i\tilde{I}_{i-1}(...),$$

where $\tilde{I}_i = I_i$ if $k_\perp^2 > \mu^2$ and $\tilde{I}_i = J_i$ if $k_\perp^2 < \mu^2$, respectively and J_i and I_i are Bessel functions for real and imaginary arguments. The series comes from the expansion of the BFKL anomalous dimension with respect to α_s. The first term of the above expansion explicitely describe BFKL dynamics in the double-logarithmic approximation:

$$\mathcal{B}(z,k_\perp^2,\mu^2) = \frac{\bar{\alpha}_S}{z\,k_\perp^2}\,J_0\left(2\sqrt{\bar{\alpha}_S\log(1/z)\log(\mu^2/k_\perp^2)}\right), \quad k_\perp^2 < \mu^2, \tag{53}$$

$$\mathcal{B}(z,k_\perp^2,\mu^2) = \frac{\bar{\alpha}_S}{z\,k_\perp^2}\,I_0\left(2\sqrt{\bar{\alpha}_S\log(1/z)\log(k_\perp^2/\mu^2)}\right), \quad k_\perp^2 > \mu^2, \tag{54}$$

where J_0 and I_0 are the standard Bessel functions (for real and imaginary arguments, respectively) and $\bar{\alpha}_S = 3\alpha_s/\pi$ is connected to the pomeron intercept Δ of the BFKL equation in LO $\omega_{\rm LL} = \bar{\alpha}_S 4\log 2$. An expression for $\omega_{\rm NLL}$ in NLO is given in [39, 40]: $\omega_{\rm NLL} = \bar{\alpha}_S 4\log 2 - N\bar{\alpha}_S^2$. Since the equations behave infrared finite no singularities will appear in the collinear approximation for small $k_\perp$.

KMR (Kimber, Martin, Ryskin [100])

In *KMR* [100] the dependence of the unintegrated gluon distribution on the two scales $k_\perp$ and μ was investigated: the scale μ plays a dual role, it acts as the factorization scale and also controls the angular ordering of the partons emitted in the evolution. Already in the case of DGLAP evolution, unintegrated parton distributions as a function of the two scales were obtained by investigating separately the real and virtual contributions to the evolution. In DGLAP the unintegrated gluon density $\mathcal{A}(x, k_\perp^2, \mu^2)$ can be written as:

$$\begin{aligned} x\mathcal{A}(x, k_\perp^2, \mu^2) &= T(k_\perp^2, \mu^2) \frac{1}{k_\perp^2} \frac{\alpha_s(k_\perp)}{2\pi} \\ &\quad \times \int_x^{(1-\delta)} P(z) x' g(x', k_\perp) dz \qquad (55) \\ &= T(k_\perp^2, \mu^2) \left. \frac{dxg(x, \mu^2)}{d\mu^2} \right|_{\mu^2 = k_\perp^2} \end{aligned}$$

where $T(k_\perp^2, \mu^2)$ is the Sudakov form factor, resumming the virtual corrections:

$$T(k_\perp^2, \mu^2) = \exp\left(- \int_{k_\perp^2}^{\mu^2} \frac{\alpha_s(k_\perp)}{2\pi} \frac{dk_\perp'^2}{dk_\perp'^2} \int_0^{(1-\delta)} P(z') dz' \right).$$

The structure of (55) is similar to the differential form of the CCFM equation in (24), but with essential differences in the Sudakov form factor as well as in the scale argument in (55). The splitting function $P(z)$ in (55) is now taken from the single scale evolution of the *unified* DGLAP-BFKL expression discussed before in *KMS* [97]. As in *KMS* the unintegrated gluon density $f(x, k_\perp^2, \mu^2)$ starts only for $k_\perp^2 > k_{\perp 0}^2 = 1$ GeV^2. An extrapolation to cover the whole range in $k_\perp^2$ has been performed [101] such, that:

$$x\mathcal{A}(x, k_\perp^2, \mu^2) = \begin{cases} \frac{xg(x, k_{\perp 0}^2)}{k_{\perp 0}^2} & \text{if } k_\perp < k_{\perp 0} \\ \frac{f(x, k_\perp^2, \mu^2)}{k_\perp^2} & \text{if } k_\perp \geq k_{\perp 0} \end{cases} \qquad (56)$$

with $xg(x, k_{\perp 0}^2)$ being the integrated MRST [102] gluon density function. The unintegrated gluon density $x\mathcal{A}(x, k_\perp^2, \mu^2)$ therefore is normalized to the MRST function when integrated up to $k_{\perp 0}^2$.

JS (Jung, Salam [14, 54])

The CCFM evolution equations have been solved numerically [14, 54] using a Monte Carlo method. The complete partonic evolution was generated according to (19–28) folded with the off-shell matrix elements for boson gluon fusion. According to the CCFM evolution equation, the emission of partons during the initial cascade is only allowed in an angular-ordered region of phase space. The maximum allowed angle Ξ for any gluon emission sets the scale $\bar{q}$ for the evolution and is defined by the hard scattering quark box, which connects the exchanged gluon to the virtual photon (see Sect. 4.2).

The free parameters of the starting gluon distribution were fitted to the structure function $F_2(x, Q^2)$ in the range $x < 10^{-2}$ and $Q^2 > 5$ GeV^2 as described in [14], resulting in the CCFM unintegrated gluon distribution $x\mathcal{A}(x, k_\perp^2, \bar{q}^2)$.

In the following we show comparisons between the different unintegrated gluon distributions. The *JS* unintegrated gluon density serves as our benchmark, because calculations based on this have shown good agreement with experimental measurements, both a HERA and at the TEVATRON. In Fig. 7 we show the gluon distributions at $\mu = \bar{q} = 10$ GeV obtained from the different BFKL sets (*KMR*, *JB*) as a function of x for different values of $k_\perp^2$ and as a function of $k_\perp^2$ for different values of x together with the *JS* unintegrated gluon density. It is interesting to note, that the *JS* gluon is less steep at small x compared to the others. However, after convolution of the *JS* gluon with the off-shell matrix element, the scaling violations of $F_2(x, Q^2)$ and the rise of F_2 towards small x is reproduced, as shown in [14, Fig. 4 therein]. In the lower part of Fig. 7, the effect of the evolution scale on the distribution in $k_\perp^2$ is shown: The *JS* and *KMR* sets both consider angular ordering for the evolution, whereas in *JB* the evolution in $k_\perp$ is decoupled from the evolution in μ, resulting in a larger $k_\perp$ tail. *JS* also includes exact energy-momentum conservation in each splitting which further suppresses the high-$k_\perp$ tail. Figure 7 also shows, that the small $k_\perp^2$ region, which essentially drives the total cross sections, is very different in different parameterizations.

In Fig. 8 we show a comparison of the gluon density distribution obtained from the derivative method (using GRV98 LO) and *KMS* and compare it to the *JS* gluon at $\bar{q} = 10$ GeV. The *KMS* and "derivative of GRV" give very similar unintegrated gluon distributions, which is a result of the strict relation between the collinear (integrated) and unintegrated gluon distributions, that was used in *KMS*. One also has to note, that *KMS* and GRV98 use very similar data sets from HERA for their fits. In Fig. 9 we show a comparison of the unintegrated gluon density parameterizations from *GBW* and *RS* and compare it to the *JS* gluon at $\bar{q} = 10$ GeV. The *RS* set is shown only for historical reasons, since it was one of the first unintegrated gluon distributions available. The *GBW* unintegrated gluon density, although successful in describing inclusive and diffractive total cross sections at HERA, is suppressed for large $k_\perp$ values (see Fig. 9), which is understandable, since large $k_\perp$ values can only originate from parton evolution, but were not treated in *GBW*. However, it is interesting to compare it also to more exclusive measurements. One can also see, that the *GBW* gluon decreases for $k_\perp \to 0$.

In Table 3 we present cross sections calculated with four of the different unintegrated gluon distributions discussed above for heavy flavor production and inclusive deep inelastic scattering at HERA energies ($\sqrt{s} = 300$ GeV) as well as the total bottom cross section at the TEVATRON. The benchmark is again the *JS* parameterization, which is able to describe the corresponding measurements at HERA and at the TEVATRON reasonably well. Large variations in the predicted cross sections are

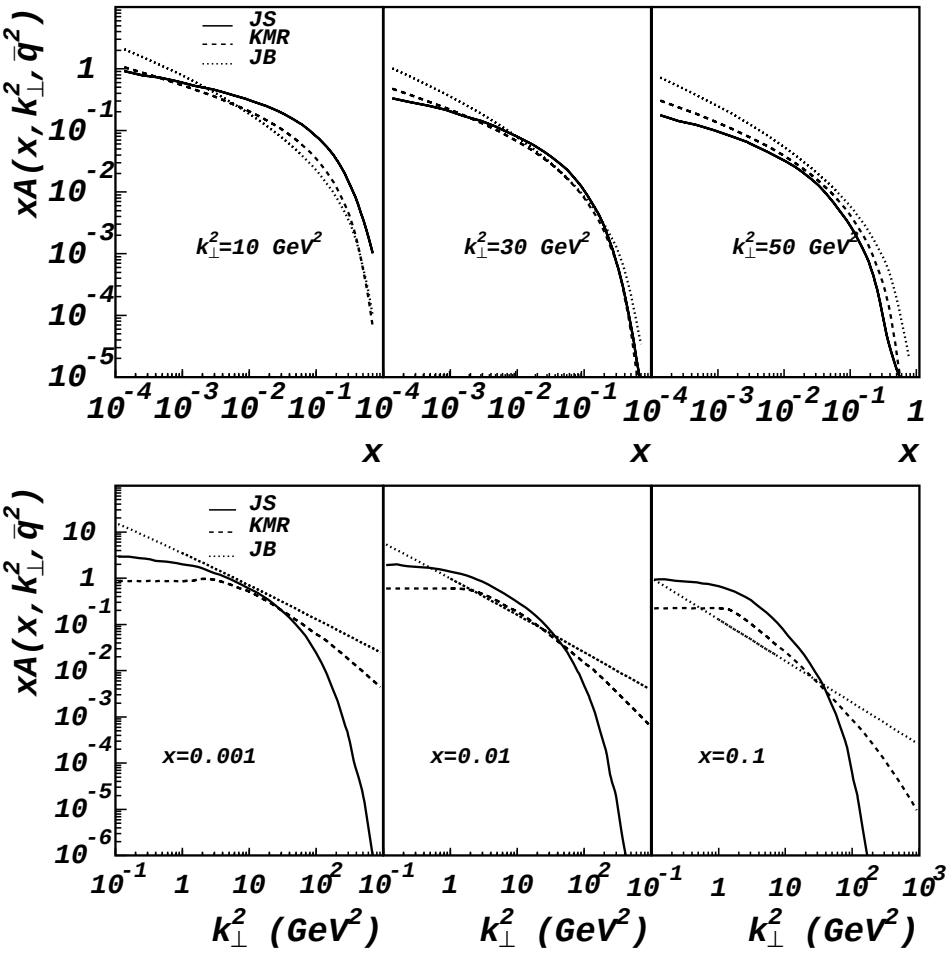

Fig. 7. The unintegrated, two scale dependent gluon distributions at $\bar{q} = \mu = 10$ GeV as a function of x for different values of $k_\perp^2$ (*upper*) and as a function of $k_\perp^2$ for different values of x (*lower*): JS [14, 54] (*solid line*), KMR [100] (*dashed line*) and JB [98] (*dotted line*)

Table 3. Cross sections for different processes at HERA and TEVATRON using different parameterizations of the unintegrated gluon distributions. The cross sections are calculated with the CASCADE [55] Monte Carlo generator. In all cases the one-loop $\alpha_s(\mu^2)$ is used with $\mu^2 = p_\perp^2 + m_q^2$, where $p_\perp$ is the transverse momentum of one of the quarks in the partonic center-of-mass frame and $m_q = 0.140, 1.5, 4.75$ GeV is mass of the light, charm and bottom quarks

	σ[nb]			
	JS	*KMR*	*JB*	*GBW*
$ep \to e' c\bar{c}X$ ($Q^2 < 1$ GeV^2)	696.8	412.8	741.3	735.3
$ep \to e' c\bar{c}X$ ($Q^2 > 1$ GeV^2)	80.2	47.4	87.7	82.0
$ep \to e' b\bar{b}X$ ($Q^2 < 1$ GeV^2)	5.36	2.78	4.38	5.64
$ep \to e' X$ ($Q^2 > 1$ GeV^2)	838.7	610.0	6550.0	4134.0
$ep \to e' X$ ($Q^2 > 5$ GeV^2)	212.8	127.2	585.1	564.0
$p\bar{p} \to b\bar{b}X$ ($\sqrt{s} = 1800$ GeV)	88100.	27489.	78934.	65990.

observed. It is clear that the parameterizations of the unintegrated gluon distributions are very poorly constrained, both theoretically and experimentally. The differences in definition makes it difficult to go beyond a purely qualitative comparison between the different parameterizations. Also, since even the integrated gluon density is only indirectly constrained by a fit to $F_2(x, Q^2)$, it may be necessary to look at less inclusive quantities to get a good handle on the unintegrated gluon.

4.6 Beyond leading logarithms

In this section the attempts to go beyond leading order are described and summarized. First, general aspects of next-to-leading effects are discussed and then the CCFM approach is critically considered,

We write the momenta of the t-channel gluons (in Sudakov representation) as $k_i = x_i^+ P_1 + x_i^- P_2 + k_{\perp i}$ and the emitted gluons as $p_i = v_i(P_1 + \xi_i P_2) + p_{\perp i}$ (20). The discussion in this section will be based on the strong ordering limit, that is x^+, angles and x^- are strongly ordered, which means that factors of $(1 - z)$ can be safely ignored since they are of $\mathcal{O}(1)$ for $z \to 0$. In the high energy limit with strong ordering, one can talk of x^+ ordering of exchanged gluons or of angular ordering of the emitted gluons. The variable ξ (related to the angle of the emitted gluons) can be written (in this approximation) as:

$$\sqrt{\xi_i} = \frac{p_{\perp i}}{x_{i-1}^+ \sqrt{s}} = \sqrt{\frac{x_{i-1}^+}{x_{i-1}^-}}, \tag{57}$$

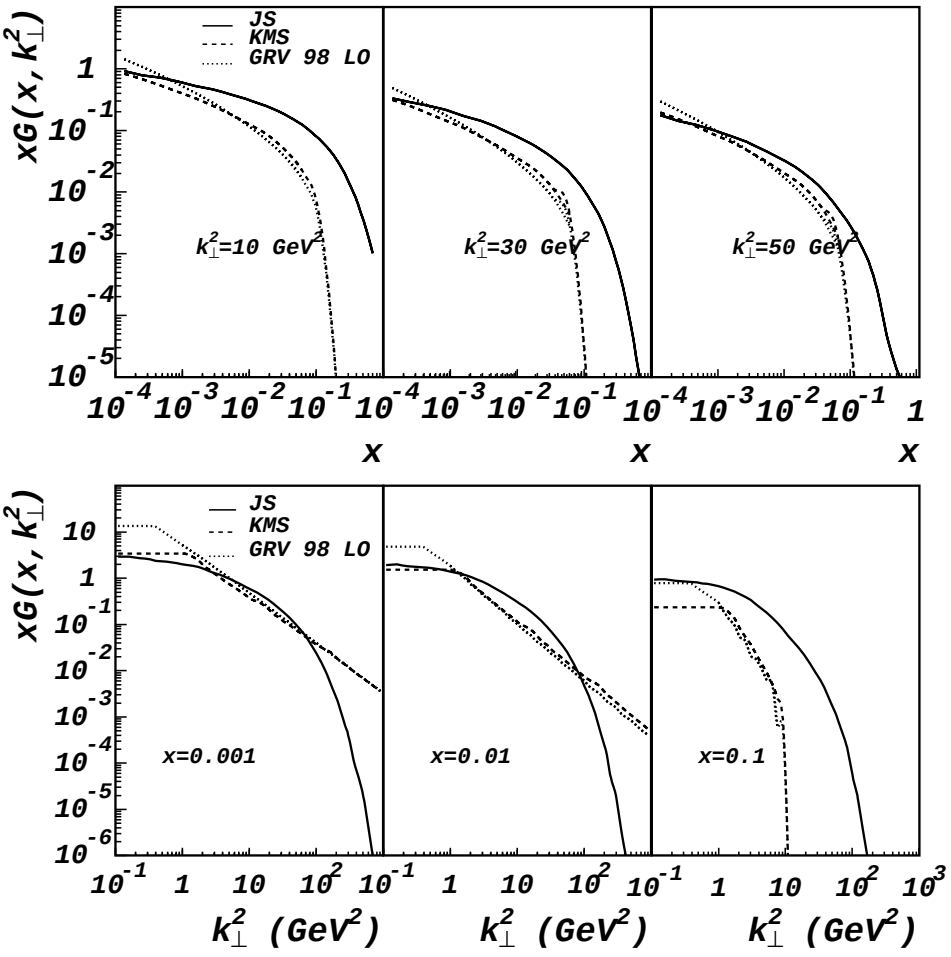

Fig. 8. The unintegrated, one scale gluon distributions as a function of x for different values of $k_\perp^2$ (*upper*) and as a function of $k_\perp^2$ for different values of x (*lower*): KMS [97] (dashed line) and derivative GRV *LO* (*dotted line*) here compared to the *two* scale gluon distribution of JS [14, 54] (*solid line*) at $\bar{q} = \mu = 10$ GeV (same as in Fig. 7)

with $v_i \sim x_{i-1}^+$ for $z \to 0$ (20). The last expression in the above equation is obtained from:

$$x_{i-1}^- \sim v_i \xi_i \sim x_{i-1}^+ \left(\frac{p_{\perp i}}{x_{i-1}^+ \sqrt{s}} \right)^2 . \qquad (58)$$

4.6.1 General next-to-leading order investigations

It is known from many contexts of QCD that for reasonably accurate predictions it is necessary (at the very least) to go to next-to-leading order. In what follows, one has to remember that the role of next-to-leading corrections in the $k_\perp$-factorization approach is very different to the ones in the collinear approach, since part of the standard NL corrections are already included at LO level in $k_\perp$-factorization, as was discussed in chapter 3.

For a next-to-leading logarithmic (NLL) calculation of a cross section at high energies, there are two main ingredients. One is the NLL corrections to the 'kernel' of the BFKL equation, generating terms $\alpha_s(\alpha_s \log 1/x)^n$. This part should be independent of the process under consideration. The second part is the correction to the impact factors (off-shell matrix elements) at either end, and is the source of the process dependence in the NLL corrections. Processes of interest include $\gamma^*\gamma^*$ scattering in electron positron annihilation, forward jets at HERA and Mueller-Navelet jets at hadron-hadron colliders. In order to describe these processes at NLO level of accuracy, one needs the photon impact factor and the jet vertex. For both elements NLO calculations are on the way: for the photon impact factor the main are the off-shell matrix elements described in Sect. 3.2 [68–70], and the quark induced jet vertex has recently been computed in [103].

One of the major developments in past years has been the completion of the calculation of the NLL corrections to the BFKL kernel. This was a significant enterprise, lasting almost a decade [39, 40]. Once the various contributions have been assembled, the final result can be given in a fairly compact form [39, 40]. It can be summarized through the following relation between the next-to-leading BFKL power, $\omega_{\rm NLL}$, and the leading power $\omega_{\rm LL} = \bar{\alpha}_{\rm S} 4 \log 2$:

$$\omega_{\rm NLL} = \bar{\alpha}_{\rm S} 4 \log 2 - N \bar{\alpha}_{\rm S}^2 \simeq \omega_{\rm LL}(1 - 6.2\alpha_s) . \qquad (59)$$

Substituting a typical value for α_s, say 0.2, one finds a negative power — so rather than improving the accuracy of the predictions, the NLL corrections seem to lead to nonsensical answers. A more detailed analysis suggests that for problems involving two substantially different transverse scales, the inclusion of the NLL corrections leads to an even worse problem, namely negative cross sections [104]. So at first sight it seems that the perturbation series

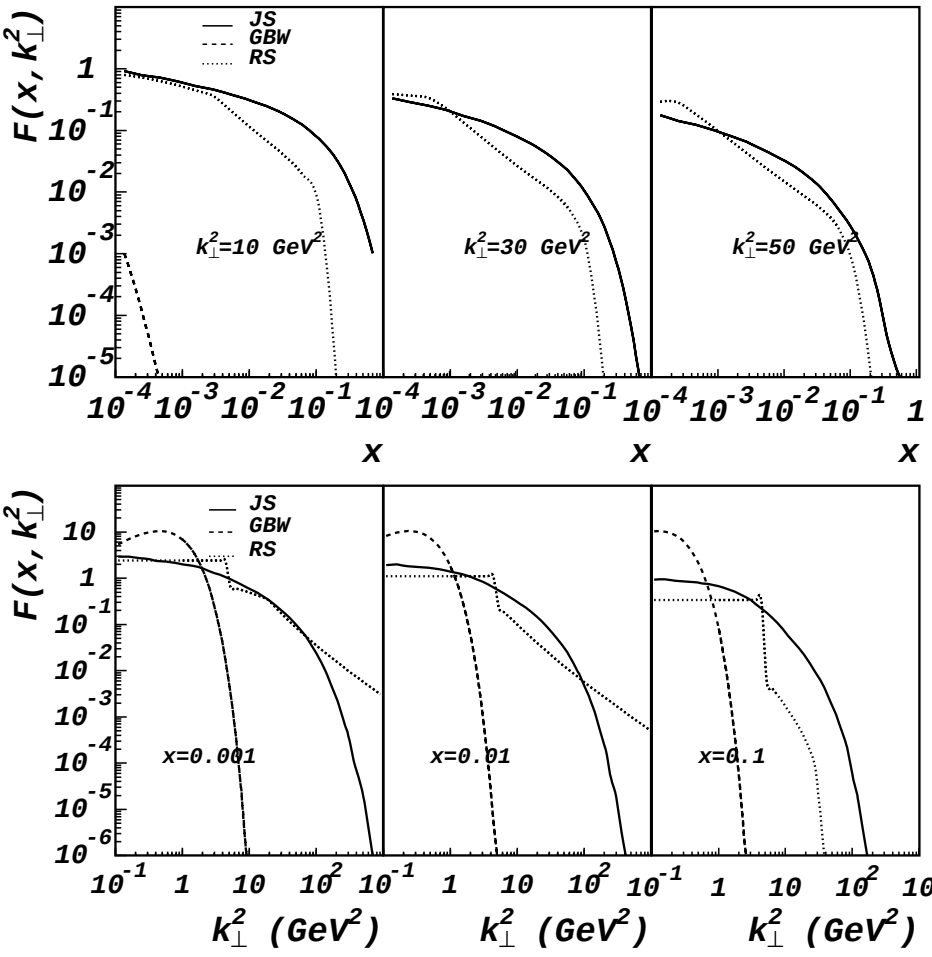

Fig. 9. The unintegrated, one scale gluon distributions as a function of x for different values of $k_\perp^2$ (*upper*) and as a function of $k_\perp^2$ for different values of x (*lower*): GBW [94] (*dashed line*) and RS [96] (*dotted line*) here compared to the *two* scale gluon distribution of JS [14, 54] (solid line) at $\bar{q} = \mu = 10$ GeV (same as in Fig. 7)

for BFKL physics is simply too poorly convergent for it to be of any practical use.

Despite this, there are indications that ways exist of using the NLL corrections for phenomenological purposes ($\gamma^*\gamma^*$, forward jets or TEVATRON jets with large rapidity separation might be examples for this). This is because it is possible to identify a well-defined physical origin for large parts of the NLL terms. These parts can then be calculated at all orders, and the remaining pieces are then a much smaller NLL correction.

A clue as to the origin of the large corrections can be obtained by examining their structure in the collinear limit (where one transverse scale is much larger than the other). From DGLAP we think we understand the origin of all terms involving $(\alpha_s \log Q^2)^n$ – they are associated with strong orderings in $k_\perp$. So e.g. in the BFKL NLO corrections (terms $\propto \alpha_s^2$) we have a piece with $(\alpha_s^2 \log^2 Q^2)$ which is something we already know about from DGLAP. Terms with this "collinear" enhancement (a number of powers of log Q) turn out to be responsible for over 90% of the NLO corrections to BFKL, and so are the reason for the large size of these corrections. But since their origin is just DGLAP physics, which we know well, we can also predict the terms that arise at NNLO $(\alpha_s^3 \log^3 Q^2)$ etc. and resum them.

Suppose one wishes to calculate the high-energy behavior of a Green's function with a squared center of mass energy s and transverse scales Q, Q_0 at the two ends of the chain. It is convenient to examine this in Mellin transform space, with ω conjugate to $s/(QQ_0)$ and γ conjugate to the squared transverse momentum ratio Q^2/Q_0^2. One can then write the BFKL kernel as

$$\omega = \bar{\alpha}_S \left(\chi_0 + \bar{\alpha}_S \chi_1 + \cdots\right), \qquad \bar{\alpha}_S = \frac{\alpha_s N_C}{\pi}. \quad (60)$$

For small γ (corresponding to a large ratio of transverse momenta) the leading part of the BFKL kernel goes as

$$\chi_0 \simeq \frac{1}{\gamma} + \mathcal{O}(\gamma^2). \quad (61)$$

In the same region the NLL corrections behave as

$$\chi_1 \simeq -\frac{1}{2\gamma^3} - \frac{11}{12\gamma^2} + \mathcal{O}(1). \quad (62)$$

The extra divergences at small γ can be quite easily understood because each power of $1/\gamma$ (after inverse Mellin transform) corresponds to a logarithm of transverse momentum ($\log Q$). So for example the term with $1/\gamma^2$, given that it multiplies α_s^2, corresponds to a contribution $(\alpha_s \log Q^2/Q_0^2)^2$, and so looks like a standard term from DGLAP evolution. One can verify the coefficient that would be expected from leading-log DGLAP evolution and it comes out as exactly $-11/12$.

The term proportional to $1/\gamma^3$ is slightly more subtle because it looks super-leading compared to DGLAP. Recalling that it is multiplied by $\bar{\alpha}_S^2$, we can see that it is related (after a Mellin transform) to a term which we can write as $(\alpha_s \log Q^2/Q_0^2) \times (\alpha_s \log^2 Q^2/Q_0^2)$, i.e. a normal DGLAP term, multiplied by a double log of Q^2. Such double logs of Q^2 will be discussed in more detail in the next subsection. Essentially, their presence or absence depends on whether we resum high energy logs of x^+, x^- or $\sqrt{x^+/x^-}$ (or equivalently Q^2/s, Q_0^2/s or QQ_0/s). The small-γ part of the NLO BFKL kernel has been shown above with the high-energy logs defined in terms of $\sqrt{x^+/x^-}$ — converting to the natural evolution variable for DGLAP evolution, x^+, the $1/\gamma^3$ pole disappears, and one is left with just the $1/\gamma^2$ term. In other words the small-γ behavior is entirely constrained by known results from DGLAP.

It is important to note though that the $1/\gamma^3$ term is not purely an artefact in that there is an analogous triple pole around $\gamma = 1$, associated with transverse logarithms for $Q_0 \gg Q$, and there is no convention for the definition of the high-energy logs which allows one to get rid of the triple poles simultaneously at $\gamma = 0$ and $\gamma = 1$.

Given that these collinearly enhanced contributions have a simple physical origin, namely the strong ordering in transverse momenta, they can be quite straightforwardly calculated not just to NLL, but to all orders. For example the generalization of the $1/\gamma^3$ and $1/(1-\gamma)^3$ terms can be obtained by implementing the kinematic constraint discussed below. The generalization of the $1/\gamma^2$ and $1/(1-\gamma)^2$ terms comes from the leading-log DGLAP kernel and from the running of the coupling.

Of course an understanding of the structure of the kernel around $\gamma = 0$ does not formally tell us anything about $\gamma = 1/2$, which is the region of interest for small-x predictions. What is remarkable though is that a collinear approximation, i.e. taking just the known poles at $\gamma = 0$ and $\gamma = 1$,

$$\chi_1^{\rm coll} = -\frac{1}{2\gamma^3} - \frac{1}{2(1-\gamma)^3} - \frac{11}{12\gamma^2} - \frac{11}{6(1-\gamma)^2}\,, \qquad (63)$$

approximates the full next-to-leading corrections to better than 93% over the whole range $0 < \gamma < 1$. The above equation is just the expression in 'γ'-space (the Mellin transform of Q space) of terms that we know from DGLAP.

This suggests that a practical approach to 'improving' NLL BFKL might just be to include the higher-order collinear terms at all orders. This has been done in [105–107], and is found to considerably improve the stability of the predictions for ω, giving a phenomenologically sensible value of ω in the range 0.25 to 0.3 for $\alpha_s \simeq 0.2$. These kinds of improvements are necessary whenever exact NLO corrections are used, because without them the result is very unstable (large renormalization scale uncertainty, negative power ω for $\alpha_s > 0.15$). The same approach can be extended to the calculation of Green's functions and physical cross sections, and work in this direction is currently in progress [108].

There have been other approaches to supplementing the NLL corrections with higher-order contributions, notably performing a BLM (Brodsky Lepage Mackenzie) change of the scale for α_s [109] and enforcing rapidity separations between emissions [110]. The basic idea behind the BLM scale choice is that a large part of the NLO corrections come about because in the LO calculation the scale choice for α_s was unreasonable. This is reflected in the NLO corrections by a large piece proportional to β_0, which is one of the parameters of the β function controlling the renormalization scale dependence of α_s. However, in a NLO calculation one obtains coefficients of n_f, and of C_A, but not of β_0 as such, so one can't identify what the actual coefficient of β_0 is. BLM identifies the "amount" of β_0 with the entire n_f part, effectively guessing from the coefficient of n_f the coefficient of β_0, and then saying that it should all be re-absorbed into a different choice of scale for α_s in the LO piece. When the authors of [109] tried this for NLO BFKL they found that it made the calculations marginally worse (even more unstable), unless they chose a very specific renormalization scheme. They argue that this scheme, which appears in certain other contexts involving three-gluon couplings (though not particularly in a small-x limit) might be a more natural choice when applying the BLM procedure, and find a value for ω of around 0.15.

The approach which enforces rapidity separations is motivated by the observation that the approximations in the LL calculation for BFKL are satisfied only when there is a large gap in rapidity between successive emissions, but that one nevertheless integrates over all possible separations between emissions (up to the limit where emissions have the same rapidity), which is plainly in violation of the initial approximations. One can choose instead to integrate up to some (a priori arbitrary) minimum rapidity separation, $\Delta\eta$. This modifies one's prediction at higher orders, and in particular can partially mimic the NLL corrections. However its explicit merging with the NLL corrections by Schmidt [110] revealed a significant remaining instability with respect to variations of $\Delta\eta$. There is evidence though that when combined with the collinear resummation described above, much of the instability with respect to the variation of $\Delta\eta$ disappears [111]. Essentially both methods (collinear enhancement, rapidity separation) cut out certain regions of phase space. With the "collinear" approach the piece cut out is well defined, whereas with the rapidity cut, the amount cut out depends on $\Delta\eta$. But when the two methods are put together, a large fraction of the phase space that would be removed by a rapidity cut has already been removed by the collinearly enhanced terms, so the effect of rapidity cut is much reduced.

4.6.2 Anomalous dimensions

So far the discussion has been most relevant to processes with two similar hard scales. In the case of re-summed small-x splitting functions (anomalous dimensions) in addition to the issues discussed above, there is a further subtlety related to *iteration* of the running of the coupling. It

has been discussed with complementary methods but similar conclusions in [107, 110, 112], [113–115] and [116]. Essentially the result is that for a small-z splitting function at scale Q^2, the typical scale in the evolution is considerably higher than Q^2 [4]. Similar results have been found before also in [120–123] in the framework of DGLAP, and in [109] in the framework of BFKL. The splitting function is only independent of Q^2 at leading order. At NLO it is no longer scale invariant because the NLO piece comes in with a different relative weight according to $\alpha_s(Q^2)$, as do NNLO etc. When deducing the small-x enhanced part of the splitting function then the NLO, NNLO, NNNLO (in the DGLAP hierarchy, $\alpha_s^{n+m}\log^n Q^2 \Rightarrow N^mLO$) pieces which are small-x enhanced need to be determined at all orders. And the final 'splitting function' then depends on Q^2 because the relative weights of all these pieces is different according to the Q^2 value. The inclusion of all these terms causes the $P_{gg}(z)$ splitting function to grow as a power $1/z^{1+\omega_c}$ at small z. Initial calculations of this dependence led to a large value for ω_c and consequent incompatibility with the data (see e.g. [124]). However these predictions are modified by two classes of large effects: NLL contributions, similar to those discussed above, and also corrections associated with the fact that the effective scale of α_s relevant to small-z splitting functions is substantially larger than Q^2. After an involved calculation one finds that, parametrically, this implies corrections to ω_c of order $\alpha_s^{5/3}, \alpha_s^{7/3}, \ldots$ (which need to be resummed) and leads to a significant reduction in the small-x power of the splitting function compared to the fixed-coupling case, as well as increased stability with respect to the NLL corrections. This means that the power ω_c for the small-z dependence of the splitting function, $1/z^{1+\omega_c}$, is smaller than one would expect (i.e. it's not the same $\omega(\alpha_s(Q^2))$ that is calculated for a process such as $\gamma^*(Q)\gamma^*(Q)$) and furthermore it sets in only at very small z (below 10^{-5}).

An approach which also involves some of the elements discussed above has been proposed and used in [125, 126] to study scaling violations in the HERA F_2 data [127]. In their approach the authors make use of a collinear resummation around $\gamma = 0$, however argue that this cannot also be applied to $\gamma = 1$, which implies that it is not possible to predict the height of the minimum of the characteristic function. Accordingly the asymptotic power λ of the small-x splitting function $\sim x^{-\lambda}$ must be fitted to the data. Within this approach the authors find an improved agreement with the F_2 data compared to a pure NLO DGLAP fit. The optimal value for λ depends on the details of how the resummation is implemented, in one case being negative ($\lambda \simeq -0.25$), while in the other it is of the order of $\lambda \simeq 0.2$ which would also be consistent with other resummation approaches.

[4] The effective high scale could be responsible (see discussions in [117–119]) for the good agreement between the experimental data for the F_2 structure function and the perturbative estimations in the small x range

4.6.3 CCFM and problems beyond leading logs

The CCFM evolution involves three partonic variables, the light-cone momentum fraction, the emission angle and the transverse momentum. Looking at the case where a forward jet in DIS has a $p_\perp^2$ much smaller than Q^2, the natural variable when going up in scale from the proton towards the virtual photon is the positive light-cone momentum fraction, $x^+ = Q^2/(sy) \sim x_{bj}$, giving rise to the standard double-logs, $\left(\bar\alpha_S \log\frac{Q^2}{p_\perp^2}\log\frac{1}{x^+}\right)^n$, coming from integrals of the form $\int_{p_\perp^2}^{Q^2} dq^2/q^2 \int_x^1 dz/z$. Naively going from the photon side with the negative light-cone momentum fraction (compare (58)) $x^- = p_\perp^2/(sy) = x^+p_\perp^2/Q^2$ will give us so-called *illegal* double-logs of $Q^2/p_\perp^2$

$$\left(\bar\alpha_S \log\frac{Q^2}{p_\perp^2}\log\frac{1}{x^-}\right)^n = \left(\bar\alpha_S \log\frac{Q^2}{p_\perp^2}\log\frac{1}{x^+} + \bar\alpha_S \log^2\frac{Q^2}{p_\perp^2}\right)^n . \quad (64)$$

The wording *illegal* comes from the observation, that the renormalization group equations (DGLAP) tell us what classes of logs we can expect (they are first order differential equations so we expect only single logs of Q^2). When we get a double log of Q^2 then this is illegal because it cannot be compatible with the renormalization group. Subtleties, of course, arise because different ways of writing the same expression can lead to the double log being visible or not, and that is what the above Eq. (64) describes. CCFM uses the angle (or more specifically ξ) as evolution variable. Using $\sqrt{\xi} = \frac{p_\perp}{x^+\sqrt{s}}$, then the ordinary collinear evolution with increasing $p_\perp$ and automatically decreasing x^+ results in angular ordering or ordering in $\sqrt{\xi}$. If on the other hand the $p_\perp$'s decrease then a decrease in x^+ does not automatically imply an increase in angle – so angular ordering becomes a stronger condition. It is the angular ordering $\sqrt{\xi} \sim \sqrt{x^+/x^-}$ which is responsible for the *illegal* double logs.

In the original formulation of CCFM a kinematic constraint was noted:

$$k_i^2 > z_{+i}k_{i-1}^2,$$

which was derived already in [128, (2.11)] and in [129] in a frame where parton i is along the z axis. If the transverse momenta $k_{\perp i}$ are to be the dominant contributions to the virtualities k_i^2 (as assumed in the derivation of the CCFM equation) then the so-called *kinematical* or *consistency constraint* is obtained:

$$k_{\perp i}^2 > z_{+i}k_{\perp i-1}^2. \quad (65)$$

To merely have a self-consistent evolution equation (no infrared unsafety, proper real-virtual cancellations), which gives correct cross sections and final-state distributions at leading logarithmic accuracy, the consistency constraint is not needed in the CCFM equation. The way the consistency constraint was originally written into the CCFM equation should not be used because it messes up real-virtual cancellations as discussed below in Sect. 4.6.4.

4.6.4 NLL corrections and event generators

There are also aspects in which the NLL corrections may be able to help guide the construction of event generators. They give a hint about the kind of physical effects which are likely to be important (splitting functions, kinematic constraint). There are also situations when building an event generator in which one is faced with two possible strategies, and sometimes the NLL corrections give clues as to the direction to be followed.

One example relates to the running of the coupling. A priori it is not necessarily clear what scale to use and for simplicity, in various phenomenological contexts, the scale has often been chosen to be $k^2_{\perp i}$ (as related to the branching $(i-1) \to i$ in Fig. 2). However, in the full NLO calculation for BFKL a term appears

$$-\bar{\alpha}_{\rm S}^2 \beta_0 \ln \frac{p^2_{\perp i}}{\mu^2} \,. \tag{66}$$

The interpretation is very simple: the right scale in the LO kernel is simply the emitted $p_\perp$ (because if included in the LO kernel and then expanded in powers of α_s, one obtains precisely such a term at NLO).

But knowledge of the 'ingredients' needed for an event generator is not always sufficient. One generally has a basic equation for the branching, such as the CCFM equation, but inserting the relevant corrections such as to obtain the correct structure of logs at the end is often not trivial, because the full set of logs comes out of the *iteration* of the branching. Furthermore some care is often needed to maintain proper cancellation of real and virtual corrections.

For example in normal BFKL the correct cubic poles around $\gamma = 1$ can be obtained by inserting the requirement $k_i^2 > z_i k_{i-1}^2$ for each branching. This corresponds to symmetrizing evolution up in transverse scale (with x^+ as the evolution variable) and evolution down in transverse scale (with x^-).

However implementing this constraint directly into CCFM leads to the wrong coefficient for the $1/(1-\gamma)^3$ term — in other words the symmetrization is not properly accomplished. One can partially solve the problem by modifying the virtual corrections (non-Sudakov) form factor

$$\ln \Delta_{ns}(z, q^2, k_\perp^2) = -\int \frac{dq'^2}{q'^2} \int_z^1 \frac{dz'}{z'} \bar{\alpha}_{\rm S}(q'^2) \Theta(q'^2 - z'^2 q^2) \times \Theta(k_\perp^2 - q'^2) \Theta\left(\frac{k_\perp^2}{q^2} - z'\right), \tag{67}$$

where the last Θ function accounts for the kinematic constraint in the virtual corrections. This will not make the cross section exactly symmetric, but it will ensure that for evolution downwards in scale the evolution variable does at least correspond roughly to x^-. On the other hand as far the final state structure is concerned, this 'hack' [130] cuts out certain regions of phase space that should be left in. An a priori way of determining whether the 'hacks' are any good should be to examine how they compare to exact NLO calculations (but that means determining their expansion to $\mathcal{O}(\alpha_s^2)$, which isn't necessarily an easy task).

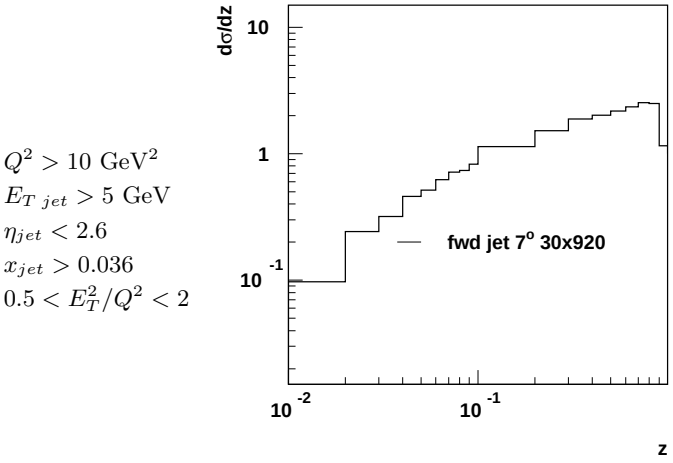

Fig. 10. The values of the splitting variable z for events satisfying the shown forward jet criteria, with $\theta = 7^o$ at HERA energies

Another source of next-to-leading-log corrections is the gluon splitting function. At very large energies, the $1/z$ term in P_{gg}, included in BFKL and CCFM, will certainly be dominant. However, the question is whether the treatment of just this term is sufficient at energies available at present colliders.

The effect of small x parton dynamics is best seen in forward jet production in deep inelastic scattering, where the contribution from typical DGLAP dynamics is suppressed. In such a process, using a Monte Carlo simulation, the distribution of z-values can be studied, and the validity of the small x approximation can be checked.

The basic event selection criteria for forward jet production at HERA are given in Fig. 10. The criterion E_T^2/Q^2 is essential to suppress the DGLAP contribution within a typical range in x of $10^{-3} < x < 10^{-2}$. The evolution takes place from the large x_{jet} down to the small x with a typical range at HERA energies of $\Delta x = x/x_{jet} > 0.01$. In order to justify the use of an evolution equation (instead of a fixed order calculation) one would require at least 2 or more gluon emissions during the evolution. To roughly estimate the energy fractions z_i of 3 gluon emissions between $10^{-3} < x < 10^{-1}$, one can assume that all gluons carry equal energies. Then the range of $\Delta x \sim 0.01$ results in $z \sim 0.2$, which is far from being in the very small z region, where the BFKL or CCFM approximations (treating only the $1/z$ terms in the gluon splitting function) are expected to be appropriate. In Fig. 10 we show the values of the splitting variable z in events satisfying the forward jet criteria at HERA energies obtained from the Monte Carlo generator CASCADE[14]. Since the values of the splitting variable z are indeed extending into the medium and large z region (the majority has $z > 0.1$), it is questionable, whether the BFKL evolution equations, including only the $1/z$ part of the gluon splitting function, are applicable. CCFM also has a $1/(1-z)$ term, which

means that in any case one expects quite a few emissions for $z \to 1$, but still, the medium z range is questionable.

The implementation of the full DGLAP splitting function into CCFM is problematic. Naively one would simply replace

$$\frac{1}{1-z} \to \frac{1}{1-z} - 2 + z(1-z)\,, \tag{68}$$

in the CCFM splitting function. However doing this leads to negative branching probabilities, so one needs to be a little more 'subtle'.

For example a positive definite branching probability can be obtained by making the following replacements

$$\begin{aligned} \frac{1}{z} &\to \frac{1-z}{z} + Bz(1-z)\,, \\ \frac{1}{1-z} &\to \frac{z}{1-z} + (1-B)z(1-z)\,, \end{aligned} \tag{69}$$

resulting in:

$$\begin{aligned} P(z,q,k) = \bar{\alpha}_{\mathrm{S}}\left(k_\perp^2\right)&\left(\frac{(1-z)}{z} + (1-B)z(1-z)\right) \\ &\times \Delta_{ns}(z,q,k) + \bar{\alpha}_{\mathrm{S}}\left((1-z)^2 q^2\right) \\ &\times \left(\frac{z}{1-z} + Bz(1-z)\right) \end{aligned} \tag{70}$$

where B is a parameter to be chosen arbitrarily between 0 and 1. As a consequence of the replacement, the Sudakov form factor will change to:

$$\begin{aligned} \log \Delta_s(\bar{q}^2, Q_0^2) = -\int_{Q_0^2}^{\bar{q}^2} \frac{dq^2}{q^2} \int_0^{1-Q_0/q} dz \bar{\alpha}_{\mathrm{S}}\left(q^2(1-z)^2\right) \\ \times \left(\frac{1-z}{z'} + (1-B)z(1-z)\right) \end{aligned} \tag{71}$$

and also the non-Sudakov form factor needs to be replaced by:

$$\begin{aligned} \log \Delta_{ns} = -\bar{\alpha}_s\left(k_\perp^2\right) \int_0^1 dz' \left(\frac{1-z}{z'} + (1-B)z(1-z)\right) \\ \times \int \frac{dq'^2}{q'^2} \Theta(k-q')\Theta(q'-z'q) \end{aligned} \tag{72}$$

which can be rewritten

$$\begin{aligned} \log \Delta_{ns} = -\bar{\alpha}_s\left(k_\perp^2\right) \int_0^1 dz' \left(\frac{1-z}{z'} + (1-B)z(1-z)\right) \\ \times 2 \ln \frac{k}{z'q} \Theta(k-z'q)\,. \end{aligned} \tag{73}$$

The proposed changes to the original CCFM splitting function are 'hacks'. There are reasonable arguments, to change the scale in α_s to $q^2(1-z)^2$ everywhere, to include the full splitting function instead of only the singular parts and also to impose the kinematic constraint, with its consequences. These 'hacks' are of course constrained by the requirement that the NLL corrections corresponding to the given branching equation are similar to the true NLL corrections. However, this will not be the real final solution and perhaps it is a need for a better starting point, embodying both angular ordering and symmetry right from the start.

5 Generators for small-x evolution

Three different Monte Carlo event generators are available, specifically devoted to small x processes (in chronological order): SMALLX [48, 49], LDCMC [50–53] and CASCADE [14, 54, 55]

5.1 SMALLX

SMALLX[48, 49] is a Monte Carlo event program which generates events on parton level at small x in ep scattering. It uses the CCFM [41–44] evolution equation for the initial state cascade convoluted with the $k_\perp$-factorized off-shell matrix elements of [35] for light and heavy quark pair production. Modifications of the original SMALLX[48, 49] version concerning the non-Sudakov form factor Δ_{ns} were necessary to obtain a reasonable description of the structure function $F_2(x, Q^2)$ as well as hadronic final states like the forward jets at HERA [54, 131].

In SMALLX the initial state gluon cascade is generated in a forward evolution approach. The gluon evolution starts from the proton side with an initial gluon distribution according to (including a Gaussian intrinsic $k_\perp$ distribution around k_0):

$$x_0 G_0(x_0, k_{\perp 0}^2) = N \cdot (1-x_0)^4 \cdot \exp\left(-k_{\perp 0}^2/k_0^2\right) \tag{74}$$

with N being a normalization constant. A gluon with momentum fraction x_i and transverse momentum $k_{\perp i}$ is allowed to branch into a virtual (t-channel) gluon with momentum k_{i+1} and a final state gluon with momentum p_{i+1} according to the CCFM splitting function [41–44]. This procedure is repeated until the next emitted gluon would violate the angular bound $\bar{q}$ given by the matrix element.

SMALLX generates the full parton level structure, but due to the complicated structure of the initial state branchings and the phase space of the matrix element, a weight is associated with each event. Although SMALLX produces weighted events and therefore is inefficient for generating specific exclusive signatures, it can be used for the CCFM evolution and to calculate the inclusive structure function $F_2(x, Q^2)$. By performing a fit to measurements of the inclusive structure function $F_2(x, Q^2)$, SMALLX can be used to determine the unintegrated CCFM gluon density $x\mathcal{A}(x, k_\perp^2, \bar{q}^2)$ in a grid in x, $k_\perp^2$ and $\bar{q}^2$ (with $\bar{q}$ being the scaled maximum angle allowed for any emission with $\bar{q}^2 = x_{n-1}^2 \Xi s$). This numerical representation can be used for any other calculation. It is advantageous, that the full parton level is generated during the evolution, since this information can be used for comparison with other event generators adopting a more efficient backward evolution approach [14, 54, 55].

5.2 CASCADE

CASCADE[14, 54, 55] is a full hadron level event generator which uses $k_\perp$-factorization of the cross section into an off-shell matrix element and an unintegrated gluon density function. The initial state cascade is generated in a

backward evolution approach, which was necessary for an efficient event generation. The Lund string fragmentation package JETSET/PYTHIA[132] is used for hadronization. CASCADE can be used in ep, γp and also $p\bar{p}$ processes.

The hard scattering process is calculated using the off-shell matrix elements given in [35] for light and heavy quark pair production, or $\gamma g \to J/\psi g$ [65] convoluted with the unintegrated gluon density $x\mathcal{A}(x, k_\perp^2, \bar{q}^2)$. It could be shown in [14, 54, 55] that a backward evolution approach [14, 54, 55, 133, 134] is possible for small x processes, which are not restricted to strong $k_\perp$ ordering in the initial state cascade. This was the main ingredient for the development of a time efficient Monte Carlo event generator.

The backward evolution starts from the hard scattering process and evolves the partons *backwards* towards the proton. This approach is much more efficient, compared to the strategy of SMALLX which uses a forward evolution approach. However, it requires the unintegrated gluon density to be determined beforehand. The CCFM unintegrated gluon distribution has been determined from a Monte Carlo solution of the CCFM evolution equation which has been fitted to the measured structure function $F_2(x, Q^2)$. It is advantageous to have the unintegrated gluon density determined in a Monte Carlo approach with full control over the partonic state, as available in SMALLX, since this allowed to show [14] that the backward evolution produces identical results to the forward evolution approach on the parton level. The proof of equivalence of the forward and backward evolution is a unique feature of CCFM. For DGLAP this has only been shown at at an inclusive level, while at the exclusive level, complications can arise related to differences in the treatment of angular ordering between forward and backward evolution.

The program code is available from
`http://www.quark.lu.se/~hannes/cascade`

5.3 LDCMC

Since the LDC model is inherently forward-backward symmetric, it is natural to design a Monte Carlo in the same way. In the LDCMC program all emissions are generated in one go from an incoming, non-perturbative gluon with energy fraction x_0, using a generating function

$$
\begin{aligned}
&G\left(a = \log\frac{Q^2 x_0}{k_{\perp 0}^2 x}, b = \log\frac{x_0}{x}\right) \qquad (75)\\
&= \sqrt{\frac{\bar{\alpha}_S a}{b}} I_1(2\bar{\alpha}_S\sqrt{ab}) = \sum_{n=1}^{\infty}\frac{\bar{\alpha}_S^n a^n b^{n-1}}{n!(n-1)!}\\
&= \sum_{n=1}^{\infty}\int \bar{\alpha}_S^n \Pi_j \frac{dz_{j+}}{z_{j+}}\frac{dz_{j-}}{z_{j-}}\delta\left(\log\frac{x}{x_0} - \sum_j \log z_{j+}\right).
\end{aligned}
$$

After this, the azimuthal angles of each emission are selected according to a flat distribution and a number of correction factors are included to produce a weight for the generated partonic state. LDCMC can either produce weighted events or use the weight as a hit-or-miss probability to produce unweighted events. The weight can include many things such as:

- The full splitting functions (also for quark propagators) instead of the simplified $\frac{dz_{j+}}{z_{j+}}\frac{dz_{j-}}{z_{j-}}$. Optionally the full matrix element for a $2 \to 2$ sub-collision can be used. In particular for the quark box closest to the virtual photon the full off-shell matrix element can be used.
- The standard Sudakov form factors.
- Emissions not satisfying the LDC constraint in (30) are given zero weight.
- The running of α_s. The scale is taken to be the transverse momentum of the emitted parton which, due to the LDC constraint, is always close to the highest scale in the emission.

Averaging over weights for a given x_0, x and Q^2, it is then possible to fit the input gluon (and quark) distribution(s) to describe eg. $F_2(x, Q^2)$.

Using these input distributions, parton-level events can be generated. Final-state parton cascades are added using the colour-dipole cascade implemented in ARIADNE for e^+e^- annihilation but only allowing emissions which are below the LDC constraint in (30). Finally, standard Lund string fragmentation can be added to produce final-state hadrons.

LDCMC is distributed together with the ARIADNE program, available from `http://www.thep.lu.se/~leif/ariadne` but in using it, one should keep in mind, that the reproduction of data on eg. forward jets is very poor. The problem can be traced to the non-singular parts of the gluon splitting function. In a newer (not yet released) version, it is possible to allow only gluonic chains and only the singular parts of the gluon splitting function. The results are then consistent with what is obtained with SMALLX and CASCADE.

6 Conclusions

In this summary report we presented the state of the art of small x physics in the year 2001. Significant progress has been made in the understanding of the small x evolution equations, CCFM and BFKL. It has been possible for the first time to describe the structure fucntion $F_2(x, Q^2)$ and also hadronic final state measurements, like forward jet production, with the CCFM evolution equation implemented into a Monte Carlo program. In more detailed studies the need for improving the small x splitting functions became evident, also from considering next-to-leading corrections to the BFKL equation. However, considering these improvements in detail, it became also clear, that this is not a trival task.

Significant progress has also been made in the understanding of $k_\perp$-factorization in general and the calculation of the off-shell matrix elements. In certain approximations the off-shell matrix elements are already calculated to order $\mathcal{O}(\alpha_s^2)$. However, some critical points still need to be

Table 4. Summary and overview over existing Monte Carlo event generators for small x physics

Name	QCD cascade	applicable	processes	event record
SMALLX [48, 49]	forward evolution with CCFM	ep	$\gamma^* g^* \to q\bar{q}$ $\gamma^* g^* \to Q\bar{Q}$	parton level weighted events
CASCADE [14, 54, 55]	backward evolution with CCFM using unintegrated gluon density	ep,γp, $p\bar{p}$	$\gamma^* g^* \to q\bar{q}$ $\gamma^* g^* \to Q\bar{Q}$ $\gamma g^* \to J/\psi g$ $g^* g^* \to q\bar{q}$ $g^* g^* \to Q\bar{Q}$	parton level unweighted events hadronization via JETSET/PYTHIA [132]
LDCMC [50–53]	forward–backward symmetric LDC evolution	ep	$\gamma^* g^* \to q\bar{q}$ $\gamma^* g^* \to Q\bar{Q}$	weighted or unweighted events final state cascade hadronization via JETSET/PYTHIA [132]

clarified, as the gauge invariance of the $k_\perp$-factorization approach is not yet clear, if considered beyond leading order.

For the first time, a comparison of all available parameterisations of unintegrated gluon distributions was made, showing significant differences, which indicate, that more (and more exclusive) measurements need to be used in constraining the unintegrated gluon distributions further. For the first time, we are in a position to try to perform a global fit, similar to those using the collinear approximation, to determine the unintegrated gluon density.

Our understanding of small-x physics is far from complete. There are a number of theoretical and phenomenological issues which need to be further settled. In this overview we have mentioned many such issues. On the theoretical side, we need to understand the convergence of the perturbative expansion of the evolution kernel, and we also need to calculate the impact factors to next-to-leading order. On the phenomenological side it is important to understand the importance of non-singular terms in the gluon splitting function especially when implemented in event generators. It is also important to understand the uncertainties involved with fitting unintegrated parton distributions to data. These parameterizations should then be compared to a wide variety of data, possibly requiring the calculation of new off-shell matrix elements for other than the mentioned processes.

Finally, we want to note that not all aspects of small-x physics have been covered in this paper. Phenomena such as rapidity gaps, shadowing effects and multiple interactions are also interesting aspects of small-x evolution, and will be included in forthcoming meetings and publications.

Appendix: The small-x collaboration

Today the work on these issues is spread out on a number of different small groups around the world. Although some of these group are already collaborating on an informal basis, it was agreed in the meeting, that the future work could be more coordinated. As a consequence of this a *Small-x Collaboration* was formed. The idea is to start small and informal and to set up a web site an a mailing list, but also to organize small meetings such as the one held in Lund resulting in this paper.

The web site is located at `http://www.thep.lu.se/Smallx` and will among other things contain a compilation of subroutines implementing parameterizations of unintegrated parton distributions and off-shell matrix elements and compilations of relevant papers, theoretical as well as phenomenological and experimental. The mailing list would be used to announce new results, to ask for help from experts in the field and so on.

The Small-x Collaboration will, of course, be open to anyone in the field. To join the collaboration one can simply join the mailing list by sending a mail to `smallx-subscribe@thep.lu.se` (more instructions can be found on the web site).

References

1. V. Gribov, L. Lipatov, Sov. J. Nucl. Phys. **15**, 438 and 675 (1972)
2. L. Lipatov, Sov. J. Nucl. Phys. **20**, 94 (1975)
3. G. Altarelli, G. Parisi, Nucl. Phys. B **126**, 298 (1977)
4. Y. Dokshitser, Sov. Phys. JETP **46**, 641 (1977)
5. E. Kuraev, L. Lipatov, V. Fadin, Sov. Phys. JETP **44**, 443 (1976)
6. E. Kuraev, L. Lipatov, V. Fadin, Sov. Phys. JETP **45**, 199 (1977)
7. Y. Balitskii, L. Lipatov, Sov. J. Nucl. Phys. **28**, 822 (1978)
8. ZEUS Collaboration; J. Breitweg et al., Eur. Phys. J. C **12**, 35 (1999), DESY 99-101
9. H1 Collaboration; C. Adloff et al., Phys. Lett. B **528**, 199 (2002), hep-ex/0108039
10. S. P. Baranov et al., A phenomenological interpretation of open charm production at HERA in terms of the semihard approach, 2002, DESY 02-017, hep-ph/0203025
11. ZEUS Collaboration; J. Breitweg et al., Eur. Phys. J. C **6**, 67 (1999)

12. S. Baranov, N. Zotov, Phys. Lett. B **458**, 389 (1999)
13. S. Baranov, H. Jung, N. Zotov, Charm production in the semi-hard approach of QCD, in Proceedings of the Workshop on Monte Carlo generators for HERA physics, edited by A. Doyle, G. Grindhammer, G. Ingelman, H. Jung (DESY, Hamburg, 1999), p. 484, hep-ph/9910210
14. H. Jung, G. Salam, Eur. Phys. J. C **19**, 351 (2001), hep-ph/0012143
15. S. Baranov, N. Zotov, Phys. Lett. B **491**, 111 (2000)
16. H1 Collaboration; C. Adloff et al., bbar in dis, in Contributed (1999)
17. ZEUS Collaboration; J. Breitweg et al., Eur. Phys. J. C **18**, 625 (2001)
18. H1 Collaboration; C. Adloff et al., Phys. Lett. B **467**, 156 (1999), and erratum ibid
19. A. V. Lipatov, V. A. Saleev, N. P. Zotov, Mod. Phys. Lett. A **15**, 1727 (2000), hep-ph/0008283
20. H. Jung, Unintegrated parton densities applied to heavy quark production in the CCFM approach, in Proceedings of the Rinberg workshop on "New trends in HERA physics", Ringberg Castle, Tegernsee, Germany. (2001), hep-ph/0109146
21. H. Jung, Phys. Rev. D **65**, 034015 (2002), DESY-01-136, hep-ph/0110034
22. ZEUS Collaboration; J. Breitweg et al., Phys. Lett. B **479**, 37 (2000)
23. H1 Collaboration, T. Ahmed et al., Eur. Phys. J. C **13**, 415 (2000), DESY 98-076 and hep-ex/9806029
24. ZEUS Collaboration; J. Breitweg et al., Eur. Phys. J. C **11**, 35 (1999), DESY 99-057
25. H1 Collaboration, C. Adloff et al., Phys. Lett. B **483**, 36 (2000)
26. H1 Collaboration, C. Adloff et al., Nucl. Phys. B **538**, 3 (1999)
27. J. Kwiecinski, A. Martin, J. Outhwaite, Eur. Phys. J. C 9 (1999) 611, hep-ph/9903439
28. H1 Collaboration; I. Abt et al., Z. Phys. C **63**, 377 (1994), DESY 94-033
29. H1 Collaboration, T. Ahmed et al., Phys. Lett. B **338**, 507 (1994)
30. A. V. Lipatov, N. P. Zotov, Mod. Phys. Lett. A **15**, 695 (2000)
31. H. Jung, Heavy quark production at HERA in k(t) factorization supplemented with CCFM evolution, 2001, hep-ph/0110345
32. R. D. Field, The sources of b-quarks at the Tevatron and their correlations, 2002, hep-ph/0201112
33. P. Hagler et al., Phys. Rev. D **62**, 071502 (2000)
34. A. V. Lipatov, V. A. Saleev, N. P. Zotov, Heavy quark production at the TEVATRON in the semihard QCD approach and the unintegrated gluon distribution, 2001, hep-ph/0112114
35. S. Catani, M. Ciafaloni, F. Hautmann, Nucl. Phys. B **366**, 135 (1991)
36. J. Collins, R. Ellis, Nucl. Phys. B **360**, 3 (1991)
37. L. Gribov, E. Levin, M. Ryskin, Phys. Rep. **100**, 1 (1983)
38. E. M. Levin, M. G. Ryskin, Y. M. Shabelski, A. G. Shuvaev, Sov. J. Nucl. Phys. **53**, 657 (1991)
39. V. S. Fadin, L. N. Lipatov, Phys. Lett. B **429**, 127 (1998), hep-ph/9802290
40. M. Ciafaloni, G. Camici, Phys. Lett. B **430**, 349 (1998), hep-ph/9803389
41. M. Ciafaloni, Nucl. Phys. B **296**, 49 (1988)
42. S. Catani, F. Fiorani, G. Marchesini, Phys. Lett. B **234**, 339 (1990)
43. S. Catani, F. Fiorani, G. Marchesini, Nucl. Phys. B **336**, 18 (1990)
44. G. Marchesini, Nucl. Phys. B **445**, 49 (1995)
45. J. R. Forshaw, A. Sabio Vera, Phys. Lett. B **440**, 141 (1998)
46. B. R. Webber, Phys. Lett. B **444**, 81 (1998)
47. G. Salam, JHEP **03**, 009 (1999)
48. G. Marchesini, B. Webber, Nucl. Phys. B **349**, 617 (1991)
49. G. Marchesini, B. Webber, Nucl. Phys. B **386**, 215 (1992)
50. B. Andersson, G. Gustafson, J. Samuelsson, Nucl. Phys. B **467**, 443 (1996)
51. B. Andersson, G. Gustafson, H. Kharraziha, J. Samuelsson, Z. Phys. C **71**, 613 (1996)
52. G. Gustafson, H. Kharraziha, L. Lönnblad, The LCD Event Generator, in Proc. of the Workshop on Future Physics at HERA, edited by A. De Roeck, G. Ingelman, R. Klanner (1996), p. 620
53. H. Kharraziha, L. Lönnblad, JHEP **03**, 006 (1998)
54. H. Jung, CCFM prediction on forward jets and F_2: parton level predictions and a new hadron level Monte Carlo generator CASCADE, in Proceedings of the Workshop on Monte Carlo generators for HERA physics, edited by A. Doyle, G. Grindhammer, G. Ingelman, H. Jung (DESY, Hamburg, 1999), p. 75, hep-ph/9908497
55. H. Jung, Comp. Phys. Comm. **143**, 100 (2002), hep-ph/0109102, DESY 01-114, `http://www.quark.lu.se/~hannes/cascade/`
56. S. Catani, Aspects of QCD, from the Tevatron to LHC, in Proceedings of the International Workshop Physics at TeV Colliders (Les Houches, France, 8-18 June, 1999), hep-ph/0005233
57. CDF Collaboration; F. Abe et al., Phys. Rev. D **55**, 2546 (1997)
58. D0 Collaboration; B. Abbott et al., Phys. Lett. B **487**, 264 (2000)
59. S. Catani, k_t-factorisation and perturbative invariants at small x, in Proceedings of the International Workshop on Deep Inelastic Scattering, DIS 96 (Rome, Italy, 15-19 April, 1996), hep-ph/9608310
60. M. G. Ryskin, A. G. Shuvaev, Y. M. Shabelski, Phys. Atom. Nucl. **64** (2001) 120
61. M. Ciafaloni, Proof of positivity of off-shell squared matrix element., private communication, 2001
62. V. Saleev, N. Zotov, Mod. Phys. Lett. A **11**, 25 (1996)
63. G. Bottazzi, G. Marchesini, G. Salam, M. Scorletti, JHEP **12**, 011 (1998), hep-ph/9810546
64. A. V. Kotikov, A. V. Lipatov, G. Parente, N. P. Zotov, The contribution of off-shell gluons to the structure functions F2(c) and F(L)(c) and the unintegrated gluon distributions, 2001, hep-ph/0107135
65. V. Saleev, N. Zotov, Mod. Phys. Lett. A **9**, 151 (1994)
66. S. Baranov, Phys. Lett. B **428**, 377 (1998)
67. S. Baranov, Matrix element for $g^*g^* \to J/\psi g$, private communication, 2001
68. J. Bartels, S. Gieseke, C. F. Qiao, Phys. Rev. D **63**, 056014 (2001), hep-ph/0009102
69. J. Bartels, S. Gieseke, A. Kyrieleis, Phys. Rev. D **65**, 014006 (2002)
70. J. Bartels, S. Gieseke, A. Kyrieleis, in preparation
71. A. H. Mueller, Nucl. Phys. B **415**, 373 (1994)

72. N. N. Nikolaev, B. G. Zakharov, V. R. Zoller, JETP Lett. **59**, 6 (1994), hep-ph/9312268
73. J. Collins, Talk presented at Lund Small x Workshop, March 2001, Lund, Sweden (unpublished)
74. J. C. Collins, D. E. Soper, Nucl. Phys. B **194**, 445 (1982)
75. J. C. Collins, D. E. Soper, Nucl. Phys. B **193**, 381 (1981), Erratum-ibid. B **213**, 545 (1981)
76. I. Balitsky, Nucl. Phys. B **463** (1996) 99
77. J. Kwiecinski, A. Martin, P. Sutton, Z. Phys. C **71**, 585 (1996)
78. Yu.L. Dokshitzer, V.A. Khoze, A.H. Mueller, S.I. Troyan, Basics of perturbative QCD (Edition Fontières, 1991)
79. R.K. Ellis, W.J. Stirling, B.R. Webber, QCD and collider physics (Cambridge University Press, 1996)
80. J. Kwiecinski, A. Martin, P. Sutton, Phys. Rev. D **52**, 1445 (1995)
81. B. Andersson, G. Gustafson, H. Kharraziha, Phys. Rev. D **57**, 5543 (1998), hep-ph/9711403
82. L. N. Lipatov, Nucl. Phys. Proc. Suppl. **99A**, 175 (2001)
83. A. V. Kotikov, L. N. Lipatov, DGLAP and BFKL evolution equations in the N = 4 supersymmetric gauge theory, 2001, DESY 02-002, hep-ph/0112346
84. A. V. Kotikov, L. N. Lipatov, 2002, in preparation
85. A. V. Kotikov, L. N. Lipatov, Nucl. Phys. B **582**, 19 (2000)
86. G. Gustafson, G. Miu, 2001, preprint in preparation
87. J. Kwiecinski, Unintegrated gluon distributions from the transverse coordinate representation of the CCFM equation in the single loop approximation, 2002, hep-ph/0203172
88. Y. L. Dokshitzer, D. Diakonov, S. I. Troian, Phys. Lett. B **79**, 269 (1978)
89. G. Parisi, R. Petronzio, Nucl. Phys. B **154**, 427 (1979)
90. J. C. Collins, D. E. Soper, G. Sterman, Nucl. Phys. B **250**, 199 (1985)
91. J. C. Collins, D. E. Soper, Phys. Rev. D **16**, 2219 (1977)
92. Y. L. Dokshitzer, D. Diakonov, S. I. Troian, Phys. Rept. **58**, 269 (1980)
93. M. A. Kimber, A. D. Martin, M. G. Ryskin, Eur. Phys. J. C **12**, 655 (2000)
94. K. Golec-Biernat, M. Wüsthoff, Phys. Rev. D **60**, 114023 (1999)
95. K. Golec-Biernat, M. Wüsthoff, Phys. Rev. D **59**, 014017 (1998)
96. M. Ryskin, Y. Shabelski, Z. Phys. C **66**, 151 (1995)
97. J. Kwiecinski, A. Martin, A. Stasto, Phys. Rev. D **56**, 3991 (1997)
98. J. Blümlein, On the k_t dependent gluon density of the proton, in Proc. of the Workshop on Deep Inelastic Scattering and QCD, edited by J. Laporte, Y. Sirois (1995), DESY 95-121 and hep-ph/9506403
99. M. Glück, E. Reya, A. Vogt, Z. Phys. C **67**, 433 (1995)
100. M. A. Kimber, A. D. Martin, M. G. Ryskin, Phys. Rev. D **63**, 114027 (2001)
101. M. Kimber, Extrapolation of unintegrated gluon density, private communication
102. A. D. Martin, R. G. Roberts, W. J. Stirling, R. S. Thorne, Nucl. Phys. Proc. Suppl. **79**, 105 (1999), hep-ph/9906231
103. J. Bartels, D. Colferai, G. P. Vacca, The NLO jet vertex for Mueller-Navelet and forward jets: The quark part, 2001, hep-ph/0112283, to be published in Phys. Rev. D
104. D. A. Ross, Phys. Lett. B **431**, 161 (1998)
105. G. Salam, JHEP. **07**, 019 (1998), hep-ph/9806482
106. M. Ciafaloni, D. Colferai, Phys. Lett. B **452**, 372 (1999)
107. M. Ciafaloni, D. Colferai, G. P. Salam, Phys. Rev. D **60**, 114036 (1999)
108. M. Ciafaloni, D. Colferai, G. Salam, A. Staśto, in preparation
109. S. J. Brodsky et al., JETP Lett. **70**, 155 (1999)
110. C. R. Schmidt, Phys. Rev. Lett. **78**, 4531 (1997)
111. J. R. Forshaw, D. A. Ross, A. Sabio Vera, Phys. Lett. B **455**, 273 (1999), hep-ph/9903390
112. M. Ciafaloni, D. Colferai, G. P. Salam, JHEP **07**, 054 (2000)
113. R. S. Thorne, Phys. Lett. B **474**, 372 (2000)
114. R. S. Thorne, Phys. Rev. D **60**, 054031 (1999)
115. R. S. Thorne, Phys. Rev. D **64**, 074005 (2001)
116. G. Altarelli, R. D. Ball, S. Forte, Nucl. Phys. B **621**, 359 (2002)
117. A. V. Kotikov, G. Parente, Nucl. Phys. B B **549**, 242 (1999)
118. A. V. Kotikov, G. Parente, Nucl. Phys. Proc. Suppl. **99A**, 196 (2001)
119. A. V. Kotikov, G. Parente, Higher twist operator effects to parton densities at small x, 2001, hep-ph/0106175
120. Y. L. Dokshitzer, D. V. Shirkov, Z. Phys. C **67**, 449 (1995)
121. A. V. Kotikov, JETP Lett. **59**, 667 (1994)
122. A. V. Kotikov, Phys. Lett. B **338**, 349 (1994)
123. W. K. Wong, Phys. Rev. D **54**, 1094 (1996)
124. S. Forte, R. D. Ball, Double scaling violations, 1996, hep-ph/9607291
125. G. Altarelli, R. D. Ball, S. Forte, Nucl. Phys. B **575**, 313 (2000), hep-ph/9911273
126. G. Altarelli, R. D. Ball, S. Forte, Nucl. Phys. B **599**, 383 (2001), hep-ph/0011270
127. H1 Collaboration, C. Adloff et al., Eur. Phys. J. C **21**, 331 (2001), hep-ex/0012053
128. A. Bassetto, M. Ciafaloni, G. Marchesini, Phys. Rep. **100**, 201 (1983)
129. M. Bengtsson, T. Sjöstrand, M. van Zijl, Z. Phys. C **32**, 67 (1986)
130. See e.g. Free On-Line dictionary of Computing, `http://wombat.doc.ic.ac.uk/foldoc/index.html`
131. H. Jung, CCFM prediction for F_2 and forward jets at HERA, in Proceedings of Workshop on Deep Inelastic Scattering and QCD (DIS 99) (DESY, Zeuthen, 1999), hep-ph/9905554
132. T. Sjöstrand, Comp. Phys. Comm. **82**, 74 (1994)
133. T. Sjöstrand, Phys. Lett. B **157**, 321 (1985)
134. M. Bengtsson, T. Sjöstrand, Z. Phys. C **37**, 465 (1988)